Digital Object Identifier

Detection, Isolation, and Magnitude Estimation of Unknown Flows in Open-Channel Irrigation Systems

GREGORY CONDE[1,2,3], NICANOR QUIJANO[2], (Senior Member, IEEE), and CARLOS OCAMPO-MARTINEZ.[3], (Senior Member, IEEE)

[1]School of Engineering, Universidad Central, Bogotá, Colombia. Email: gcondem@ucentral.edu.co
[2]School of Engineering, University of Los Andes, Bogotá, Colombia. Email: nquijano@uniandes.edu.co
[3]Automatic Control Department, Universitat Politècnica de Catalunya, Institut de Robòtica i Informàtica Industrial (CSIC-UPC) Barcelona, Spain. Email: carlos.ocampo@upc.edu

Corresponding author: Gregory Conde (e-mail: gcondem@ucentral.edu.co).

This research has been supported by Séptima Convocatoria Interna de Investigación de la Universidad Central, Convocatoria Proyectos de Investigación Conjunta Universidad de Ibagué-Universidad de los Andes (2019-2021), and the CSIC Project MuYSCA (Ref. COOPA20246).

ABSTRACT The development of modeling and estimation strategies, useful for determining the magnitude and location of unknown flows such as seepage and leaks, appears as a valuable tool to increase the efficiency of the open-channel irrigation systems (OCIS). However, it has been identified that in OCIS, most of the strategies reported on detection, isolation, and magnitude estimation of unknown flows (DIMEUF) have been developed from linear models that do not include information about energy balances along the channels, where these balances are fundamental to differentiate changes of levels due to conduction effects, from changes of levels due to unknown flows. Therefore, in this work, a recent OCIS modeling approach, which includes mass and energy balances for each channel and non-linear hydraulic descriptions of the flows, is explored in the development of two strategies for DIMEUF based on the moving horizon estimation (MHE) approach. The first strategy is deterministic, designed under the assumption that by filtering of the measurements, the noise can be sufficiently attenuated. Therefore, the noise information is not included in the design process. On the other hand, the second strategy is stochastic, and includes remaining noise information in the design process. The developed strategies have been tested using data from a testbed implemented in a specialized software, and the results show that, in a large operation region, the proposed strategies are capable of accurately describe the channel behavior and unknown flows, and that the inclusion of the remaining noise information increases the performance of the strategies for DIMEUF.

INDEX TERMS Unknown flows, Leaks, Seepage, Estimation, Open channel, Irrigation systems, Open canal

I. INTRODUCTION

In agriculture, the easiest and most cost-efficient way to transport water is through open-channel irrigation systems (OCIS). In this process, water is taken from a natural source and transported by networks of OCIS. Despite that irrigation is known as the activity that most water consumes, these systems generally present low efficiency [1], and the major source of losses is produced by leaks [2]. Therefore, the opportune detection, isolation, and magnitude estimation of unknown flows (DIMEUF) such as seepage and leaks is an alternative to take actions that might reduce losses. In OCIS, multiple works have been reported around the field of fault diagnosis and DIMEUF [3]–[15]. These works highlight the importance in the selection of an appropriate modeling approach, which is fundamental in the development of strategies for detection and estimation of unknown variables. For example, as emphasized in [8], the DIMEUF strategies designed from linear models [3], [4], [6], [11]–[16] are only valid close to an operation region. Hence, in order to increase this region, some works have explored the development of DIMEUF strategies using non-linear models such as numerical solutions of the Saint-Venant Equations (SVE) and approximated models. The approximated models are those developed from basic physical principles, observations,

and empirical knowledge of the OCIS (e.g., integrator-delay model, gray-box models, and linear-parameter variance). In contrast, the SVE are used to obtain fundamental models that can offer an accurate analytical description of the water behavior for infinitesimal sections of the channels. In reported works that have designed DIMEUF strategies using approximated models [5], [8]–[10], it is found that the approximated models do not contemplate energy balances along the channels, and this could lead to inaccurate DIMEUF. For example, in [6] strategies for magnitude estimation of unknown flows are tested in a real system, reporting drift in the results, concluding that this drift is due to the growth of weeds, which affects the flow conduction. Moreover, the OCIS are usually affected by sedimentation that also changes the resistance and conduction offered along the channels. Meanwhile, in reported works that design DIMEUF strategies from numerical solutions of the SVE, the complexity of the algorithm is one of the key aspects, obtaining algorithms that: i) only detects or isolates [7]; or ii) algorithms where the estimation process must be performed off-line [9].

Alternatively, in [17] a new and intuitive approximated modeling approach that combines mass and energy balances has been proposed. This modeling approach includes the nonlinear hydraulic relationships that characterize the OCIS, showing an accurate behavior in a broad operation region. Furthermore, it has been identified that the moving horizon estimation (MHE) is known for its inherent capability of handling complex nonlinear systems and let the inclusion of additional physical information of the system by the use of constraints [18]. Hence, in this work, the use of the model presented in [17] is considered in the development of a MHE strategy for OCIS. In this direction, it has been identified that: i) in order to obtain accurate estimations of the unknown flows magnitude, the MHE strategy must be enhanced with the addition of detection and isolation mechanisms; and ii) in the OCIS high inflow or outflow variations produce small level variations of the system, and the unknown flows can easily be masked into small variations of level measurements (i.e, noise measurement). Therefore, in the design of strategies for DIMEUF rigorous noise analysis must be performed.

In this order of ideas, the main contributions of this work are twofold. First, we propose a new approach for DIMEUF in OCIS, which, takes into account the effects of flow conduction and is developed by enhancing an MHE approach with the inclusion of detection and isolation mechanisms. Then, from the proposed estimation approach, a stochastic DIMEUF strategy that contemplates the effects of noise measurement is also proposed. A comparative analysis that contextualizes the proposed strategies for DIMEUF is presented in Table 1. In this table, the different modeling, flow description, and estimation strategies reported in the literature are contrasted with the strategies proposed in this work. This table highlights that, by using a no-linear modeling strategy that contemplates conduction effects along the OCIS, the proposed strategies, let the online detection, isolation, and magnitude estimation of the unknown flows, and cover the multiple gaps that in mater of DIMEUF have been identified.

The remainder of the paper is organized as follows. Section II starts with a summary of the estimation modeling strategy, and describes the problem of accurate unknown flows magnitude estimations by using an MHE approach. In Section III, first, a deterministic MHE strategy enhanced with detection and isolation mechanisms is proposed as a solution in getting accurate magnitude estimations of the unknown flows; and second, the deterministic strategy is extended with the development of a stochastic strategy that includes measurement noise information. In Section IV the implementations of the deterministic and stochastic approaches are explained and validated by using the testbed proposed in [19], which is implemented in the stormwater management model (SWMM) software. In Section V the simulation results are presented and discussed. Finally, in Section VI some conclusions are drawn.

II. PROBLEM STATEMENT

A rigorous analytical description of the OCIS dynamics is given by the Saint-Venant equations (SVE), which are two non-linear partial differential equations that relate mass and momentum conservation for each infinitesimal section of the OCIS [20]. However, the direct use of the SVE for control systems and estimation design is impractical [21]. In order to address this issue, multiple control-oriented models have been reported in the literature. In [22] an overview of the reported control-oriented models is given, where these models have been classified in: i) models that come from analytical simplifications of the SVE (simplified models); and, ii) models that come from approximations, observations, and assumptions of the dynamic behavior of the OCIS (approximated models). In the simplified models, most of the nonlinear OCIS relations are neglected during the simplification process, where linearization procedures are usually performed. On the other hand, in most approximated models the potential energy balance along the channels is avoided, and this balance is important to relate level changes due to conduction changes, and level changes due to seepage and leaks. In this work, this problem is overcome by using the modeling approach presented in [17], which describes the nonlinear dynamical behavior of the OCIS by using mass and energy balances. Therefore, this modeling strategy is presented and employed in the development of an estimation model, which is used to show the problem in getting optimal solutions by applying a conventional MHE strategy.

A. MODELING APPROACH

As it is shown in Fig. 1, i corresponds to the stage number (e.g., $i = 1$ denotes the first channel), and each channel is analyzed as two storage units with areas a_{up_i} for the upstream unit, and a_{dn_i} (m^2) for the downstream unit, where the size of the respective areas can be obtained using identification techniques. In this model, the channel p_i is fed by the flow q_i (m^3/s) that comes from the upstream canal p_{i-1}. Besides, x_{up_i} and x_{dn_i} (m) are the depth at

TABLE 1. Comparison between reported approaches for detection, isolation, and magnitude estimation of unknown flows in OCIS.

Work	*Estimation Model*	*Flow Description*	*Estimation Strategy*	*Detection*	*Isolation*	*Estimation*	*Conduction*	*Online*	*Nonlinear Modeling*
[3]	Integrator delay	Linear flow relation	Bank of unknown-input observers	✓	✓			✓	
[4]	Integrator delay	Linear flow relation	Bank of unknown-input observers	✓	✓			✓	
[5]	Grey-box	Nonlinear flow relation	Discrepancies between model and real system	✓				✓	✓
[6]	Linearized SVE	Linear flow relation	i) Detection of measurement deviations ii) Kalman filter	✓	✓		✓	✓	
[7]	Numerical solutions of the SVE	Linear flow relation	i) Discrepancies between model and real system ii) Bank of linear observers	✓	✓		✓	✓	✓
[8]	Linear parameter variance	Nonlinear flow relation	Discrepancies between model and real system	✓	✓			✓	✓
[9]	i) Grey-box ii) Numerical solutions of the SVE	Nonlinear flow relation	i) Discrepancies between model and real system ii) Extended Kalman filter iii) Heuristic strategy	✓	✓	✓	✓		✓
This paper	Mass and energy balances	Nonlinear flow relation	i) Deterministic MHE-detection, isolation, & MHE-Estimation mechanisms ii) Stochastic MHE-detection, isolation, & MHE-Estimation mechanisms	✓	✓	✓	✓	✓	✓

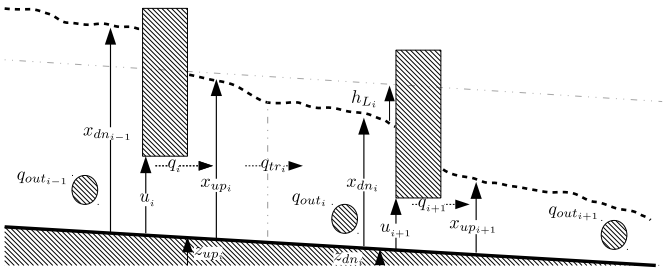

Fig. 1. Graphical description of the proposed energy and mass balances.

the upstream and downstream end, respectively. From the channel p_i, there could be multiple outflows to other channels or users. However, the outflows have been simplified into the outlet flow to the users q_{out_i} and the flow that feeds the downstream channel q_{i+1}. In OCIS, the inflows and outflows have an hydraulic relationship with the corresponding regulation structures, which could be classified into gates (Fig. 2) and weirs (Fig. 3) that regulate in either free-flow or submerged-flow configurations [23]. Table 2 summarizes the mathematical relationships for the discharge through each kind of regulation structure, where w_i (m) is the width of the regulation structure, g (m/s^2) is the gravity constant, c_i (with corresponding dimensions) is the discharge coefficient, and u_i (m) is the position of the regulation structure.

Flow Transition

The modeling strategy assumes a flow transition $q_{tr_i}(t)$ (m^3/s) between the two storage units. This flow is obtained from an energy balance along the channel, which is given by

$$z_{up_i} + x_{up_i} + \frac{{v_{up_i}}^2}{2g} = z_{dn_i} + x_{dn_i} + \frac{{v_{dn_i}}^2}{2g} + h_{L_i}, \tag{1}$$

TABLE 2. Flow relation for different categories of regulation structures

	Free-flow
Gate	$q_i = c_i w_i u_i \sqrt{2g}\sqrt{x_{dn_{i-1}} - 0.5u_i}$
Weir	$q_i = c_i w_i \sqrt{2g}(x_{dn_{i-1}} - u_i)^{3/2}$
	Submerged-flow
Gate	$q_i = c_i w_i u_i \sqrt{2g}\sqrt{x_{dn_{i-1}} - x_{up_i}}$
Weir	$q_i = c_i w_i \sqrt{2g}(x_{dn_{i-1}} - x_{up_i})^{3/2}$

where the difference between z_{up_i} and z_{dn_i} is the potential energy related to the channel inclination, v_{up_i} and v_{dn_i} are the upstream and downstream mean flow velocities, $\frac{{v_{up_i}}^2}{2g}$ and $\frac{{v_{dn_i}}^2}{2g}$ are the kinetic energies at the upper and lower part of the channel. Besides, h_{L_i} is known as the head loss due to friction, which can be described by the Darcy-Weisbach equation [24]. In this model, equal mean flow velocity along the channel is assumed. Moreover, in this model, the head loss due to friction is assumed to be a function of: i) the

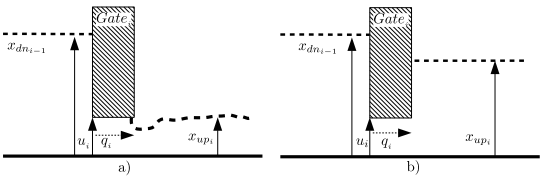

Fig. 2. Flow relation for: a) Gate in free-flow. b) Gate in submerged-flow.

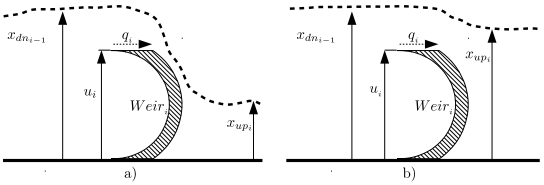

Fig. 3. Flow relation for: a) Weir in free-flow. b) Weir in submerged-flow.

upstream level; ii) the flow transition between the two storage unities ($q_{tr_i}(t)$); and iii) a transition constant k_{tr_i}, which could be obtained from experimental tests, and is related to both channel dimensions (diameter, length, and width), and conduction conditions (friction factor). Then, assuming that $h_{L_i} \approx \frac{q_{tr_i}^2}{{k_{tr_i}}^2 x_{up_i}^2}$, and performing the energy balance proposed in (1), the flow transition is given by

$$q_{tr_i}(t) = k_{tr_i}(t) x_{up_i}(t) \sqrt{x_{up_i}(t) - x_{dn_i}(t) + z_{up_i} - z_{dn_i}}. \tag{2}$$

Unknown Flows

In this paper, the problems associated with DIMEUF, such as seepage and leaks, are considered. In OCIS, leaks can be given by accidental losses of water through orifices. A common example of a leak is illustrated by [5], describing a gate letting water through, even when it is fully closed. Another example can be given when water percolates through channel fissures. In these cases, such losses can be modeled as functions of the level, where these unknown flows are localized, i.e., $\kappa_{m_i}(t) g(x_{m_i}(t))$, where x_{m_i} is the level at the m_i^{th} position and κ_{m_i} is a parameter related to the size of the orifice or fissures aperture [25]. In this paper, the hydraulic description of an unknown flow at the upstream part of the channel i is expressed as

$$s_{up_i}(t) = \kappa_{up_i}(t) \sqrt{x_{up_i}(t)}, \;\; \kappa_{up_i}(t) \geq 0, \tag{3}$$

where $\kappa_{up_i}(t)$ is a parameter that could suddenly change and is associated with the upstream orifice aperture. The hydraulic description of a leak at the downstream part of the channel is expressed as

$$s_{dn_i}(t) = \kappa_{dn_i}(t) \sqrt{x_{dn_i}(t)}, \;\; \kappa_{dn_i}(t) \geq 0, \tag{4}$$

where $\kappa_{dn_i}(t)$ is the parameter associated with the downstream orifice aperture.

Simulation Model

Once the flows that affect the OCIS have been defined, a model of the system can be obtained by performing a mass balance for each storage unit, obtaining a model described as

$$a_{up_i} \dot{x}_{up_i}(t) = q_i(t) - q_{tr_i}(t) - s_{up_i}(t) \tag{5a}$$
$$a_{dn_i} \dot{x}_{dn_i}(t) = q_{tr_i}(t) - q_{out_i}(t) - q_{i+1}(t) - s_{dn_i}(t) \tag{5b}$$
$$y_{up_i}(t) = x_{up_i}(t) \tag{5c}$$
$$y_{dn_i}(t) = x_{dn_i}(t), \tag{5d}$$

where $y_{up_i}(t) \geq 0$ and $y_{dn_i}(t) \geq 0$ are the measured upstream and downstream levels, respectively. Flows $q_i(t) \geq 0$, $q_{i+1}(t) \geq 0$, and $q_{out_i}(t) \geq 0$ can be obtained by measuring the levels associated with the respective regulation structure (see Table 2). At this point, a nonlinear control-oriented modeling approach designed from mass and approximated potential energy balances for each channel has been presented. The modeling approach (5) can be categorized as a grey-box model, where its structure is obtained from knowledge about the system's behavior, and parameters associated to the flows $q_i(t)$, $q_{i+1}(t)$, and $q_{out_i}(t)$ can be obtained from physical features of the real system. On the other hand, the parameters that cannot be obtained from physical dimensions, such as the upstream and downstream areas (a_{up_i}, and a_{dn_i}), the transition constant (k_{tr_i}), and the parameters associated to the upstream and downstream leaks or seepage (κ_{up_i}, and κ_{dn_i}) can be obtained through either data fitting or estimation. In this work, the upstream and downstream areas are considered time-invariant, and are obtained by formulating a data fitting problem, where, if the absence of unknown flows and reduced noise measurements is assumed, the unknown flow transition can be neglected by the addition of the two mass balances that describe the system (5), which, by using an Euler method, can be discretized yielding to

$$\begin{aligned}&\frac{a_{up_i}}{\tau_s}(x_{up_i}(k+1)-x_{up_i}(k))+\\&\frac{a_{dn_i}}{\tau_s}(x_{dn_i}(k+1)-x_{dn_i}(k))\\&=q_i(k)-q_{out_i}(k)-q_{i+1}(k).\end{aligned}\tag{6}$$

Therefore, the upstream and downstream model areas are obtained by solving the optimization problem given by

$$\begin{aligned}&\min_{\theta_{a_i}} \quad \|\phi_{x_i}\theta_{a_i}-y_{q_i}\|^2\\&\text{s.t.}\\&a_{up_i}+a_{dn_i}=a_i,\end{aligned}\tag{7}$$

where for an experiment with n data,

$$\phi_{x_i}=\begin{bmatrix}\frac{x_{up_i}(k+1)-x_{up_i}(k)}{\tau_s} & \frac{x_{dn_i}(k+1)-x_{dn_i}(k)}{\tau_s}\\ \frac{x_{up_i}(k+2)-x_{up_i}(k+1)}{\tau_s} & \frac{x_{dn_i}(k+2)-x_{dn_i}(k+1)}{\tau_s}\\ \vdots & \vdots\\ \frac{x_{up_i}(k+n)-x_{up_i}(k+n-1)}{\tau_s} & \frac{x_{dn_i}(k+n)-x_{dn_i}(k+n-1)}{\tau_s}\end{bmatrix},$$

$$y_{q_i}=\begin{bmatrix}q_i(k)-q_{out_i}(k)-q_{i+1}(k)\\ q_i(k+1)-q_{out_i}(k+1)-q_{i+1}(k+1)\\ \vdots\\ q_i(k+n-1)-q_{out_i}(k+n-1)-q_{i+1}(k+n-1)\end{bmatrix},$$

and $\theta_{a_i}=[a_{up_i}\quad a_{dn_i}]^\top$. Here, the constraint $a_{up_i}+a_{dn_i}=a_i$ is included to ensure that the overall area of the approximated model is equal to the physical system area. As it can be seen, this modeling strategy presents some important qualities that in the estimation approach are exploited: i) with the modeling strategy an exact overall mass balance for each channel can be guaranteed; ii) the dynamic behavior of the model can be tuned by adjusting the upstream and downstream areas with real data; iii) the upstream and downstream channel levels can be used in the nonlinear hydraulic description of inflows and outflows of interacting channels; and iv) the nonlinear descriptions of the inflows and outflows can be integrated into the estimation model, increasing the operation region where this model is valid. Note that the upstream and downstream areas have been considered as time-invariant identified parameters. On the other hand, k_{tr_i}, κ_{up_i}, and κ_{dn_i} are parameters that can change due to sedimentation, and incorrect gate closing, or a sudden channel fissure. Therefore, an estimation model is developed in order to consider the online estimation of such parameters.

Estimation Model

At this point, the OCIS can be modeled using two non-linear differential equations that describe mass and energy balances for each channel. Now, with the objective to develop a strategy for DIMEUF, by using an Euler discretization method, the modeling approach (5) is used in the development of a discrete-time estimation model as follows:

$$\begin{aligned}\hat{x}_{up_i}(k+1)=&\hat{x}_{up_i}(k)+\frac{\tau_s}{a_{up_i}}(q_i(k)-\hat{q}_{tr_i}(k)-\hat{s}_{up_i}(k)),\\ \hat{x}_{dn_i}(k+1)=&\hat{x}_{dn_i}(k)+\frac{\tau_s}{a_{dn_i}}(\hat{q}_{tr_i}(k)-q_{out_i}(k)\\&-q_{i+1}(k)-\hat{s}_{dn_i}(k)),\end{aligned}\tag{8}$$

where τ_s (s) is the sampling time; $\hat{x}_{up_i}(k)\geq 0$, $\hat{x}_{dn_i}(k)\geq 0$, $\hat{q}_{tr_i}(k)\geq 0$, $\hat{s}_{up_i}(k)\geq 0$, and $\hat{s}_{dn_i}(k)\geq 0$, are considered unknown variables to be estimated. These variables correspond to the upstream level, the downstream level, the flow transition, and the upstream and downstream leaks, respectively. In contrast, the flows $q_i(k)\geq 0$, $q_{out_i}(k)\geq 0$, and $q_{i+1}(k)\geq 0$ are considered known variables that can be obtained from measurements of the real system. A compact description of the discrete-time estimation model (8) is given by

$$\begin{aligned}\hat{x}_i(k+1)&=G_i\hat{x}_i(k)+H_i\hat{\psi}_i(k)+H_{f_i}\xi_i(k),\\ \hat{y}_i(k)&=\hat{x}_i(k),\end{aligned}\tag{9}$$

where the variables correspond to: the vector of unknown states $\hat{x}_i(k)=[\hat{x}_{up_i}(k)\ \hat{x}_{dn_i}(k)]^\top$; the vector of unknown flows to be estimated $\hat{\psi}_i(k)=[\hat{q}_{tr_i}(k)\ \hat{s}_{up_i}(k)\ \hat{s}_{dn_i}(k)]^\top$; the vector of known flows $\xi_i(k)=[q_i(k)\ q_{out_i}(k)\ q_{i+1}(k)]^\top$; and the vector of unknown outputs to be estimated $\hat{y}_i(k)=[\hat{y}_{up_i}(k)\ \hat{y}_{dn_i}(k)]^\top$. The state matrix, the unknown flows matrix, and the known flows matrix are given by

$$G_i=\begin{bmatrix}1&0\\0&1\end{bmatrix},\ H_i=\begin{bmatrix}-\frac{\tau_s}{a_{up_i}} & -\frac{\tau_s}{a_{up_i}} & 0\\ \frac{\tau_s}{a_{dn_i}} & 0 & -\frac{\tau_s}{a_{dn_i}}\end{bmatrix},\text{ and}$$

$$H_{f_i}=\begin{bmatrix}\frac{\tau_s}{a_{up_i}} & 0 & 0\\ 0 & -\frac{\tau_s}{a_{dn_i}} & -\frac{\tau_s}{a_{dn_i}}\end{bmatrix},$$

respectively.

Note that, according to the hydraulic descriptions of the unknown flows given in (2), (3), and (4), the vector of unknown flows $\hat{\psi}_i(k)$ can be described as a linear combination of known or measured variables and unknown parameters as

$$\hat{\psi}_i(k)=\Omega_i(k)\hat{\theta}_i(k),\tag{10}$$

where $\Omega_i(k)\in\mathbb{R}^{3\times 3}$ is a matrix of hydraulic relations that can be obtained from measurements of the real system by

$$\Omega_i(k)=\begin{bmatrix}\gamma_i(k) & 0 & 0\\ 0 & \sqrt{y_{up_i}(k)} & 0\\ 0 & 0 & \sqrt{y_{dn_i}(k)}\end{bmatrix},$$

$$\gamma_i(k)=y_{up_i}(k)\sqrt{y_{up_i}(k)-y_{dn_i}(k)+z_{up_i}-z_{dn_i}},$$

and $\hat{\theta}_i(k)\in\mathbb{R}^3$ is a vector of time-varying unknown parameters to be estimated, described as

$\hat{\theta}_i(k)=[\hat{k}_{tr_i}(k)\ \hat{k}_{up_i}(k)\ \hat{k}_{dn_i}(k)]^\top$.

These unknown parameters are associated to real and non-negative physical variables such as areas and conduction coefficients (i.e., $\hat{k}_{tr_i}(k)$, $\hat{k}_{up_i}(k)$, $\hat{k}_{dn_i}(k)\geq 0$). This is important information that must be included into the estimation strategies.

B. MHE PROBLEM

In order to estimate the vector of unknown parameters $\hat{\theta}_i(k)$, the MHE strategy is considered. This is an optimization-based estimation strategy that consists in minimizing a cost function defined over a receding time window of inputs and outputs data with fixed length [26]. This technique is known for its inherent capability of handling complex nonlinear systems with constraints [18], showing that it could be a suitable strategy to deal with the estimation problem in OCIS. However, following, it is shown that the direct use of the MHE strategy leads to inaccurate estimations of the unknown parameters. As it is shown in Figure 4, in the MHE strategy an estimation window with length N_h that starts in $N_{hp}=k-N_h+1$ and ends in k is established. Note that the notation $\hat{y}_i(k\mid N_{hp})$ indicates that the data $\hat{y}_i(k)$ depends on the conditions at the time N_{hp}. Over this window, the estimation of the model (8) is given by

$$\hat{\boldsymbol{y}}_i=\boldsymbol{\Phi}_i\hat{x}_i(N_{hp}\mid N_{hp})+\boldsymbol{B}_i\boldsymbol{\Omega}_i(k)\hat{\boldsymbol{\theta}}_i(k)+\boldsymbol{B}_{f_i}\boldsymbol{\xi}_i(k),\tag{11}$$

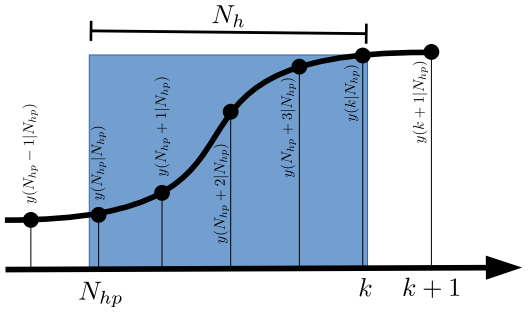

Fig. 4. Graphical description of data over an estimation window.

where

$$\begin{aligned}
\hat{\boldsymbol{y}}_i =&[\hat{y}_i(N_{hp}+1 \mid N_{hp})^\top \quad \hat{y}_i(N_{hp}+2 \mid N_{hp})^\top \\
&\cdots \quad \hat{y}_i(k+1 \mid N_{hp})^\top]^\top, \\
\boldsymbol{\Phi}_i =&[(G_i)^\top \quad (G_i^2)^\top \quad \cdots \quad (G_i^{N_h})^\top]^\top, \\
\boldsymbol{B}_i =&\begin{bmatrix} H_i & \mathbf{0} & \cdots \\ G_iH_i & H_i & \cdots \\ \vdots & \vdots & \vdots \\ \boldsymbol{G}_i^{N_h-1}H_i & \boldsymbol{G}_i^{N_h-2}H_i & \cdots \end{bmatrix}, \\
\boldsymbol{\Omega}_i(k) =&\text{diag}(\Omega_i(N_{hp} \mid N_{hp}) \quad \Omega_i(N_{hp}+1 \mid N_{hp}) \\
&\cdots \quad \Omega_i(k \mid N_{hp})), \\
\hat{\boldsymbol{\theta}}_i(k) =&[\hat{\theta}_i(N_{hp} \mid N_{hp})^\top \quad (\hat{\theta}_i(N_{hp}+1 \mid N_{hp}))^\top \\
&\cdots (\hat{\theta}_i(k \mid N_{hp}))^\top]^\top \\
\boldsymbol{B}_{f_i} =&\begin{bmatrix} H_{f_i} & \mathbf{0} & \cdots \\ G_iH_{f_i} & H_{f_i} & \cdots \\ \vdots & \vdots & \vdots \\ G_i^{N_h-1}H_{f_i} & G_i^{N_h-2}H_{f_i} & \cdots \end{bmatrix}, \\
\boldsymbol{\xi}_i(k) =&[\xi_i(N_{hp} \mid N_{hp})^\top \quad (\xi_i(N_{hp}+1 \mid N_{hp}))^\top \\
&\cdots (\xi_i(k \mid N_{hp}))^\top]^\top,
\end{aligned}$$

with $\hat{\boldsymbol{y}}_i \in \mathbb{R}^{2N_h}$, $\boldsymbol{\Phi}_i \in \mathbb{R}^{2N_h \times 2}$, $\boldsymbol{B}_i \in \mathbb{R}^{2N_h \times 3N_h}$, $\boldsymbol{\Omega}_i(k) \in \mathbb{R}^{3N_h \times 3N_h}$, $\hat{\boldsymbol{\theta}}_i(k) \in \mathbb{R}^{3N_h}$, $\boldsymbol{B}_{f_i} \in \mathbb{R}^{2N_h \times 3N_h}$, $\boldsymbol{\xi}_i(k) \in \mathbb{R}^{3N_h}$, and $\mathbf{0}$ a null matrix with appropriate dimensions.

In order to find the estimated parameters $\hat{\boldsymbol{\theta}}_i(k)$ that minimizes the deviation between estimated and measured levels, first, the development of a conventional MHE strategy is formulated. A block diagram of the MHE strategy is shown in Fig. 5, where additionally to the estimation model and the optimization stage, it is taken into account that the known flow measurements $\xi(k)$ and the known hydraulic relations $\Omega_i(k)$ are obtained from levels measurements and positions of the regulation structures (Table 2). Also, it is assumed that the level measurements are performed using ultrasound sensors, and these measurements should be sampled and filtered. Therefore, a low-pass filter stage and a sampling stage are included. As a result, as long as the noise is sufficiently attenuated (in the estimation mechanism), the proposed objective function to be minimized can be given by

$$\boldsymbol{V}_i = \|\boldsymbol{y}_i - \hat{\boldsymbol{y}}_i\|^2_{\mathcal{R}_{1_i}} + \|\hat{\boldsymbol{\theta}}_i(k-1) - \hat{\boldsymbol{\theta}}_i(k)\|^2_{\mathcal{R}_{2_i}}, \tag{12}$$

where $\boldsymbol{y}_i$ is a vector of the measured levels given by

$$\begin{aligned}
\boldsymbol{y}_i =&[y_i(N_{hp}+1 \mid N_{hp})^\top \quad y_i(N_{hp}+2 \mid N_{hp})^\top \\
&\cdots \quad y_i(k+1 \mid N_{hp})]^\top,
\end{aligned}$$

with $\boldsymbol{y}_i \in \mathbb{R}^{2N_h}$. In (12), the term $\|\hat{\boldsymbol{\theta}}_i(k-1) - \hat{\boldsymbol{\theta}}_i(k)\|^2_{\mathcal{R}_{2_i}}$ is included as a forgetting factor that takes into account the influence of past estimations [27], where $\hat{\boldsymbol{\theta}}_i(k-1)$ is the sequence of unknown parameters estimated in a previous iteration. Moreover, $\mathcal{R}_{1_i} \in \mathbb{R}^{2N_h \times 2N_h}$ and $\mathcal{R}_{2_i} \in \mathbb{R}^{3N_h \times 3N_h}$ are diagonal and positive definite weighting matrices that penalize the estimation error and the forgetting factor, respectively. The constraints inclusion is used to add information to the estimation problem [28], then, as the unknown parameters must be positive, the minimization problem is proposed as

$$\begin{aligned}
&\min_{\hat{\boldsymbol{\theta}}_i(k)} \quad \boldsymbol{V}_i \\
&\text{s.t.} \\
&\hat{\boldsymbol{\theta}}_i(k) \geq 0.
\end{aligned} \tag{13}$$

Note that the reachability of suitable sequences of the unknown parameters ($\hat{\boldsymbol{\theta}}_i(k)$) depends on the convexity of the objective function (12). In Lemma 1, it is shown that the use of a conventional MHE strategy does not guarantee an optimal estimation of $\hat{\boldsymbol{\theta}}_i(k)$.

Lemma 1. *From the objective function (12), only sub-optimal estimations of $\hat{\boldsymbol{\theta}}_i(k)$ can be reached.*

Proof. A necessary condition for any local minimum to be a global minimum is the convexity of the objective function (12). This condition can be reached if the Hessian with respect to $\hat{\boldsymbol{\theta}}_i(k)$ is positive definite, i.e.,

$$\nabla^2_{\hat{\boldsymbol{\theta}}_i(k)} \boldsymbol{V}_i = \boldsymbol{\Omega}_i(k)^\top \boldsymbol{B}_i^\top \mathcal{R}_{1_i} \boldsymbol{B}_i \boldsymbol{\Omega}_i(k) + \mathcal{R}_{2_i} \succ \mathbf{0}. \tag{14}$$

Since $\mathcal{R}_{1_i}$ and $\mathcal{R}_{2_i}$ are positive defined, the condition established in (14) is achieved if $\boldsymbol{\Omega}_i(k)^\top \boldsymbol{B}_i^\top \boldsymbol{B}_i \boldsymbol{\Omega}_i(k) \succ \mathbf{0}$.

A sufficient condition for $\boldsymbol{\Omega}_i(k)^\top \boldsymbol{B}_i^\top \boldsymbol{B}_i \boldsymbol{\Omega}_i(k) \succ \mathbf{0}$ is that the rank of $\boldsymbol{B}_i \boldsymbol{\Omega}_i(k)$ should be equal to $3N_h$. But, given the dimensions of $\boldsymbol{B}_i$ and $\boldsymbol{\Omega}_i(k)$, the maximum rank of $\boldsymbol{B}_i \boldsymbol{\Omega}_i(k)$ is $2N_h$. Therefore, the condition (14) and an optimal estimation of $\hat{\boldsymbol{\theta}}_i(k)$ cannot be reached.

However, by definition, $\boldsymbol{\Omega}_i(k)^\top \boldsymbol{B}_i^\top \boldsymbol{B}_i \boldsymbol{\Omega}_i(k)$ is positive semi-definite [29], then, the term

$$\boldsymbol{\Omega}_i(k)^\top \boldsymbol{B}_i^\top \mathcal{R}_{1_i} \boldsymbol{B}_i \boldsymbol{\Omega}_i(k)$$

is positive semi-definite.

Therefore, the Hessian $\nabla^2_{\hat{\boldsymbol{\theta}}_i(k)} \boldsymbol{V}_i$ is positive semi-definite and only sub-optimal estimations of $\hat{\boldsymbol{\theta}}_i(k)$ can be guaranteed. □

A contextualized explanation of the problem can be synthesized in that the minimization of the error between the upstream and downstream levels can be reached with inaccurate combinations of the estimated unknown flows. Therefore, if only an unknown flows estimation algorithm is used, inaccurate estimations of the unknown parameters can be reached.

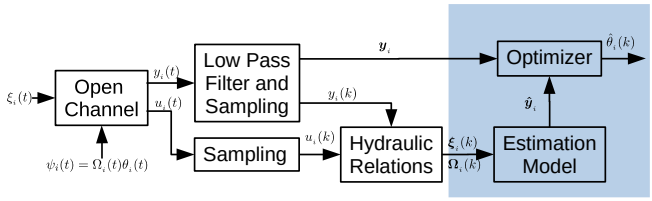

Fig. 5. Estimation mechanism.

According to the approximate model order (5), the maximum rank of $\boldsymbol{B}_i$ is $2N_h$. Therefore, if only two unknown inputs are considered, the convexity of the objective function can be guaranteed. For the two inputs case, H_i is in $\mathbb{R}^{2\times 2}$, and the rank of $\boldsymbol{B}_i$ is still $2N_h$. This solution can be reached by estimation of the total amount of the upstream unknown flows ($-q_{tr_i}(t) - s_{up_i}(t)$) and the total amount of the downstream unknown flows ($q_{tr_i}(t) - s_{dn_i}(t)$). Then, by direct addition of the upstream and downstream unknown flows, the total amount of unknown flows that affect an open-channel can be estimated. This problem is solved in [30] by using an MHE strategy. Other strategies such as unbiased minimum-variance state estimation [31], and state estimators with quadratic boundedness [32] could be explored to solve this issue. However, by using the two unknown-inputs consideration, the upstream and downstream origins of the unknown flows cannot be established. Therefore, as a proposed solution, following, an enhanced strategy that includes detection and isolation mechanisms is proposed.

III. PROPOSED APPROACH

In order to overcome the non-convex estimation problem, in Fig. 6 an enhanced strategy for DIMEUF is proposed, where: i) the detection mechanism uses information about variations of the known flows ($\Delta\xi_i(k)$) and variations of the measured levels ($\Delta y_i(k+1)$) to estimate variations of the unknown flows ($\Delta\hat{\psi}_i(k)$); ii) in the isolation mechanism, the information about the estimated variations of the unknown flows are used to establish the origin of the unknown flow, which can be an either upstream or downstream unknown flow; and iii) in the estimation algorithm, the forgetting factor of the unlikely unknown flow is penalized in order to estimate the flow transition and the corresponding unknown flow that minimizes the objective function (12).

Next, deterministic and stochastic analyses of the proposed strategies are performed. The deterministic analysis is developed assuming that the noise can be sufficiently attenuated by the filtering stage. On the other hand, the stochastic analysis is developed including information about remaining measurement noise that can affect the detection, isolation, and estimation processes.

A. DETERMINISTIC APPROACH

Note that under the assumption that the measurement noise can be sufficiently attenuated, the difference between the estimation mechanisms (Figures 5 and 6) is that in the proposed strategy for DIMEUF the weighting matrix that penalizes the forgetting factor ($\mathcal{R}_{2_i}(k)$) is time variant. This weighting matrix is adjusted by the isolation mechanism, which receives information from the detection mechanism as it is described next.

Detection Mechanism

The proposed detection mechanism is developed using a similar MHE strategy than the developed for the estimation mechanism, with the difference that in the detection strategy, the objective is to estimate the variations of the unknown flows. Therefore, from the proposed estimation model (9), a variational estimation model is derived as

$$\begin{aligned}\Delta\hat{x}_i(k+1) =& G_i\Delta\hat{x}_i(k) + H_i\Delta\hat{\psi}_i(k) + H_{f_i}\Delta\xi_i(k)\\ \Delta\hat{y}_i(k) =& \Delta\hat{x}_i(k),\end{aligned} \tag{15}$$

where, $\Delta\hat{x}_i(k+1) = \hat{x}_i(k+1) - \hat{x}_i(k)$; $\Delta\hat{\psi}_i(k) = \hat{\psi}_i(k) - \hat{\psi}_i(k-1)$; and $\Delta\xi_i(k) = \xi_i(k) - \xi_i(k-1)$. Note that the variational estimation model maintains the same state and input matrices than the estimation model (9). Therefore, over an estimation window, the variational estimation model is given by

$$\Delta\hat{\boldsymbol{y}}_i = \boldsymbol{\Phi}_i\Delta\hat{x}_i(N_{hp} \mid N_{hp}) + \boldsymbol{B}_i\Delta\hat{\boldsymbol{\psi}}_i(k) + \boldsymbol{B}_{f_i}\Delta\boldsymbol{\xi}_i(k),$$

where

$$\begin{aligned}\Delta\hat{\boldsymbol{y}}_i =& [\Delta\hat{y}_i(N_{hp}+1 \mid N_{hp})^\top \quad \Delta\hat{y}_i(N_{hp}+2 \mid N_{hp})^\top\\ & \cdots \quad \Delta\hat{y}_i(k+1 \mid N_{hp})^\top]^\top,\\ \Delta\hat{\boldsymbol{\psi}}_i(k) =& [\Delta\hat{\psi}_i(N_{hp} \mid N_{hp})^\top \quad \Delta\hat{\psi}_i(N_{hp}+1 \mid N_{hp})^\top\\ & \cdots \Delta\hat{\psi}_i(k \mid N_{hp})^\top]^\top.\\ \Delta\boldsymbol{\xi}_i(k) =& [\Delta\xi_i(N_{hp} \mid N_{hp})^\top \quad \Delta\xi_i(N_{hp}+1 \mid N_{hp})^\top\\ & \cdots \Delta\xi_i(k \mid N_{hp})^\top]^\top,\end{aligned}$$

with $\Delta\hat{\boldsymbol{y}}_i \in \mathbb{R}^{2N_h}$, $\Delta\hat{\boldsymbol{\psi}}_i(k) \in \mathbb{R}^{3N_h}$, $\Delta\boldsymbol{\xi}_i(k) \in \mathbb{R}^{3N_h}$.

In the detection strategy, the objective is to find the vector of variations of the unknown flows ($\Delta\hat{\boldsymbol{\psi}}_i(k)$) that minimizes the quadratic error between the variations of the measured levels ($\boldsymbol{\Delta y}_i$) and the variations of the estimated levels ($\boldsymbol{\Delta\hat{y}}_i$). Therefore, it is proposed to minimize the cost function given by

$$\boldsymbol{J}_i = \|\boldsymbol{\Delta y}_i - \boldsymbol{\Delta\hat{y}}_i\|^2_{\mathcal{D}_{1_i}} + \|\boldsymbol{\Delta\hat{\psi}}_i(k-1) - \boldsymbol{\Delta\hat{\psi}}_i(k)\|^2_{\mathcal{D}_{2_i}}, \tag{16}$$

where the vector of variations of the measured levels is given by

$$\begin{aligned}\Delta\boldsymbol{y}_i =& [\Delta y_i(N_{hp}+1 \mid N_{hp})^\top \quad \Delta y_i(N_{hp}+2 \mid N_{hp})^\top\\ & \cdots \Delta y_i(k+1 \mid N_{hp})^\top]^\top.\end{aligned}$$

Besides, $\|\Delta\hat{\boldsymbol{\psi}}_i(k-1) - \Delta\hat{\boldsymbol{\psi}}_i(k)\|^2_{\mathcal{D}_{2_i}}$ is included as a forgetting factor, and $\Delta\hat{\boldsymbol{\psi}}_i(k-1)$ is the vector of variations of unknown flows estimated in a previous iteration. Moreover, $\mathcal{D}_{1_i} \in \mathbb{R}^{2N_h\times 2N_h}$ and $\mathcal{D}_{2_i} \in \mathbb{R}^{3N_h\times 3N_h}$ are diagonal and positive definite weighting matrices that penalize the variational estimation error and the forgetting factor, respectively.

Isolation Mechanism

As it is shown in Fig. 6, the proposed isolation mechanism uses unknown flows estimated variations ($\Delta\hat{\boldsymbol{\psi}}_i(k)$) to establish the possible origin of the unknown flow and penalizes the corresponding forgetting factor of the unlikely unknown flow. This is developed under the following assumption.

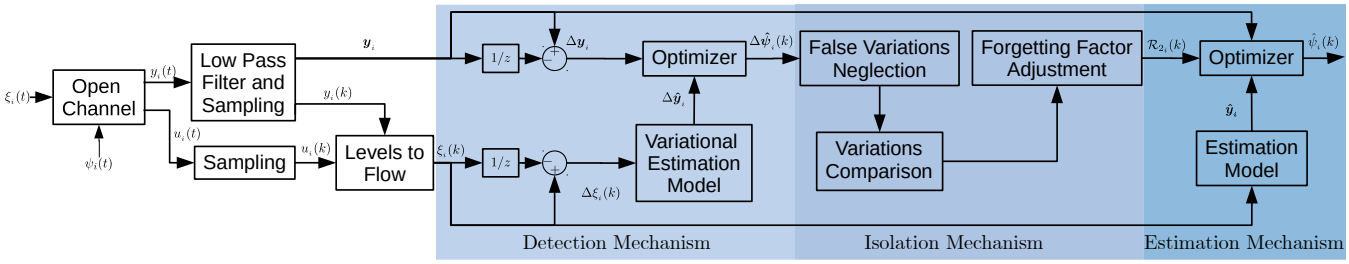

Fig. 6. Proposed detection, isolation, and estimation mechanisms.

Assumption 1 (No simultaneous variations of leaks)**.** *In an open-channel, upstream and downstream variations of unknown flows do not coincide at the same time.*

Based on Assumption 1, the isolation mechanism can be described as a signal comparison mechanism, where: i) a threshold value (Λ_{Δ_i}) is established in order to discriminate between noise and real variations of unknown flows; ii) the magnitudes of the estimated upstream and downstream variations of unknown flows are compared in order to establish the feasible origin of the variation; and iii) in the objective function of the estimation mechanism (12), the diagonal weighting matrix is transformed into a dynamic matrix that penalizes the forgetting factor $\mathcal{R}_{2_i}(k)$. Therefore, the forgetting factor is adjusted as $\mathcal{R}_{2_i}(k) = \text{diag}(\mathcal{R}_{ktr_i}(k) \quad \mathcal{R}_{kup_i}(k) \quad \mathcal{R}_{kdn_i}(k) \quad \dots \quad \mathcal{R}_{kdn_i}(k))$, and the isolation mechanism modifies $\mathcal{R}_{ktr_i}(k)$, $\mathcal{R}_{kup_i}(k)$, and $\mathcal{R}_{kdn_i}(k)$ as follows:

- if an upstream unknown flow variation is most likely, then $\mathcal{R}_{ktr_i}(k) = \alpha_i, \mathcal{R}_{kup_i}(k) = \alpha_i, \mathcal{R}_{kdn_i}(k) = \beta_i$;
- if a downstream unknown flow variation is most likely, then $\mathcal{R}_{ktr_i}(k) = \alpha_i, \mathcal{R}_{kup_i}(k) = \beta_i, \mathcal{R}_{kdn_i}(k) = \alpha_i$;

where, if $\beta_i >> \alpha_i$, the change of the unlikely unknown parameter is avoided, and the minimization of the objective function of the estimation mechanism (12) is performed by $k_{tr_i}(k)$ and the unknown parameter of the origin of the variation $k_{up_i}(k)$ or $k_{dn_i}(k)$.

Estimation Mechanism

Finally, the information of the isolation mechanism is included in the cost function of the estimation mechanism as follows:

$$\boldsymbol{V}_i = \|\boldsymbol{y}_i - \hat{\boldsymbol{y}}_i\|^2_{\mathcal{R}_{1_i}} + \|\hat{\boldsymbol{\theta}}_i(k-1) - \hat{\boldsymbol{\theta}}_i(k)\|^2_{\mathcal{R}_{2_i}(k)}. \tag{17}$$

The cost function is minimized in order to obtain the magnitudes of the estimated parameters $\hat{k}_{tr_i}(k)$ $\hat{k}_{up_i}(k)$, and $\hat{k}_{dn_i}(k)$. Note that the magnitude of leaks and seepage can be obtained by linear combinations of the estimated parameters and functions of the upstream and downstream measured levels (10).

B. STOCHASTIC APPROACH

Even though the deterministic approach contemplates noise reduction with the inclusion of a low-pass filter, the remaining measurement noise can affect the detection, isolation, and estimation processes. Therefore, in this section, mechanisms that maximize the likelihood detection and likelihood estimation of the unknown flows are designed. The stochastic approach maintains the same detection, isolation, and estimation sequence of the deterministic approach (see Fig. 6). However, for the sake of simplicity, the stochastic estimation mechanism is discussed first, and then the stochastic detection and isolation mechanisms are addressed.

Stochastic Estimation Mechanism

In the stochastic estimation mechanism, the remaining measurement noise after filtering is considered. Moreover, as the known inputs q_i, q_{out_i}, and q_{i+1} are obtained from measurements of the levels (see Table 2), the remaining measurement noise can also affect the model dynamics. Consequently, an estimation model that includes remaining measurement noise information can be stated by

$$\begin{aligned} \hat{x}_i(k+1) =& G_i\hat{x}_i(k) + H_i\hat{\psi}_i(k) + H_{f_i}\xi_i(k) + \omega_i(k), \\ \hat{y}_i(k) =& \hat{x}_i(k) + \nu_i(k), \end{aligned} \tag{18}$$

where $\omega_i(k) = [\omega_{up_i}(k) \quad \omega_{dn_i}(k)]^\top$ is the process estimation noise, $\omega_{up_i}(k)$, and $\omega_{dn_i}(k)$ are normally distributed noise, with zero mean and standard deviation $\sigma_{\omega up_i}$ and $\sigma_{\omega dn_i}$, respectively. Similarly, $\nu_i(k) = [\nu_{up_i}(k) \; \nu_{dn_i}(k)]^\top$ is the remaining measurement noise, with zero mean and standard deviation $\sigma_{\nu up_i}$ and $\sigma_{\nu dn_i}$, respectively.

In order to consider the remaining measurement noise, and the expected values of the levels, the estimation is performed under the following assumption.

Assumption 2 (Expected estimated levels)**.** *Over an estimation window, the expected values of $\boldsymbol{y}_i$ can be estimated from*

$$\begin{aligned} \hat{\bar{\boldsymbol{y}}}_i =& \boldsymbol{\Phi}_i\hat{x}_i(N_{hp} \mid N_{hp}) + \boldsymbol{B}_i\boldsymbol{\Omega}_i(k)\boldsymbol{T}_i\hat{\bar{\theta}}_i(k) \\ &+ \boldsymbol{B}_{f_i}\boldsymbol{\xi}_i(k) + \boldsymbol{W}_i(k) + \boldsymbol{N}_i, \end{aligned} \tag{19}$$

where $\hat{\bar{\boldsymbol{y}}}_i \in \mathbb{R}^{2N_h}$ is the vector of estimated expected values of the output, $\hat{\bar{\theta}}_i(k) = [\hat{\bar{k}}_{tr_i}(k) \; \hat{\bar{k}}_{up_i}(k) \; \hat{\bar{k}}_{dn_i}(k)]^\top \in \mathbb{R}^3$ are the expected values of the unknown parameters, and $\boldsymbol{T}_i \in \mathbb{R}^{3N_h \times 3}$ is a block of identity matrices such that $\boldsymbol{T}_i\hat{\bar{\theta}}_i(k) \in \mathbb{R}^{3N_h}$. Finally, $\boldsymbol{W}_i(k) \in \mathbb{R}^{2N_h}$ and $\boldsymbol{N}_i \in \mathbb{R}^{2N_h}$ are the corresponding process and measurement noise vectors, respectively.

It is emphasized that additionally to the noise inclusion, the deterministic and stochastic cases (Equations (11) and (19)), differ in the configuration of the unknown parameters. Note that in (11), $\hat{\boldsymbol{\theta}}_i(k) \in \mathbb{R}^{3N_h}$ is the estimated unknown parameters for each instant of the estimation window. In contrast, in (19), it is considered that the unknown parameters ($\hat{\bar{\theta}}_i(k) \in \mathbb{R}^3$) are the same over the entire estimation window. In that form, in the stochastic estimation mechanism, the objective is to find the unknown parameters ($\hat{\bar{\theta}}_i(k)$) that makes the vector of measured levels $\boldsymbol{y}_i$ most likely. For that a likelihood function must be established, where over an estimation window, the process covariance can be obtained from the estimation error $e_i = y_i(k+1) - \hat{\bar{y}}_i(k+1)$, and the covariance is the expected value given by

$$P_i(k+1) = \mathbb{E}\left(e_i(k+1)e_i(k+1)^\top\right). \tag{20}$$

Consequently, if a discrete model of the system is given by

$$\begin{aligned} x_i(k+1) =& G_i x_i(k) + H_i\psi_i(k) + H_{f_i}\xi_i(k), \\ y_i(k) =& x_i(k), \end{aligned} \tag{21}$$

and if the unknown flows ($\psi_i(k)$) are considered to be zero or identical to the unknown estimated flows ($\hat{\psi}_i(k)$), by subtraction, from (18) and (21), the estimated error can be written as

$$e_i(k+1) = G_i e_i(k) + \omega_i(k) + \nu_i(k+1).$$

Therefore, from (20), the process covariance is given by

$$P_i(k+1) = G_i P_i(k) G_i^\top + R + S, \tag{22}$$

where

$$R = \begin{bmatrix} \sigma^2_{\omega up_i} & 0 \\ 0 & \sigma^2_{\omega dn_i} \end{bmatrix}, \; S = \begin{bmatrix} \sigma^2_{\nu up_i} & 0 \\ 0 & \sigma^2_{\nu dn_i} \end{bmatrix}.$$

Finally, the process covariance (22) is given by

$$\begin{aligned} \boldsymbol{\Sigma}_i(k) = &\text{diag}[(P_i(N_{hp} \mid N_{hp}), P_i(N_{hp}+1 \mid N_{hp}), \cdots \\ &P_i(k \mid N_{hp}))]. \end{aligned} \tag{23}$$

The process covariance contains information about the deviation that the expected values present over an estimation window. Next, the process covariance is included in the development of the likelihood function used to find the expected values of $\hat{\bar{\theta}}_i(k)$. Then given the process covariance (23) and the estimation process (19), a probability density function (likelihood function) can be formulated as

$$f(\boldsymbol{y}_i \mid \hat{\bar{\boldsymbol{\theta}}}_i(k)) = \frac{1}{(2\pi)^{N_h} \left|\boldsymbol{\Sigma}_i(k)\right|^{1/2}} e^{-\frac{1}{2}\boldsymbol{\Upsilon}}, \tag{24}$$

where

$$\boldsymbol{\Upsilon} = (\boldsymbol{y}_i - \hat{\bar{\boldsymbol{y}}}_i)\boldsymbol{\Sigma}_i(k)^{-1}(\boldsymbol{y}_i - \hat{\bar{\boldsymbol{y}}}_i).$$

Now, the goal is to find the estimated values $\hat{\bar{\theta}}_i(k)$ that makes the measured vector ($\boldsymbol{y}_i$) most likely. Therefore, the probability density function (24) must be maximized with respect to $\hat{\bar{\theta}}_i(k)$. However, as it is shown in [33], for the sake of simplicity, the logarithm of (24) can be maximized leading to the following minimization problem:

$$\underset{\hat{\bar{\theta}}_i(k)}{\text{minimize}} \quad \boldsymbol{\Upsilon}. \tag{25}$$

Similarly to the deterministic case, in the objective function, in order to retain influence of past estimations, also the forgetting factor ($\|\hat{\bar{\theta}}_i(k-1) - \hat{\bar{\theta}}_i(k)\|^2_{\mathcal{R}_{s_i}}$) can be included, leading to the cost function

$$\boldsymbol{V}_{s_i} = \|\boldsymbol{y}_i - \hat{\bar{\boldsymbol{y}}}_i\|^2_{\boldsymbol{\Sigma}_i(k)^{-1}} + \|\hat{\bar{\theta}}_i(k-1) - \bar{\theta}_i(k)\|^2_{\mathcal{R}_{s_i}(k)}, \tag{26}$$

where $\mathcal{R}_{s_i}(k) \in \mathbb{R}^{3\times 3}$ is used to penalize the forgetting factor. Moreover, if constraints on the unknown parameters are included, the minimization problem of the estimation mechanism is formulated as

$$\begin{aligned} &\min_{\hat{\bar{\theta}}_i(k)} \quad \boldsymbol{V}_{s_i} \\ &\text{s.t.} \\ &\hat{\bar{\theta}}_i(k) \geq 0. \end{aligned} \tag{27}$$

Note that by following a similar analysis as in Lemma 1, the convexity of the stochastic objective function (26) can be reached if the rank of $\boldsymbol{B}_i\boldsymbol{\Omega}_i(k)\boldsymbol{T}_i$ is $3N_h$, but given the dimensions of $\boldsymbol{B}_i$, $\boldsymbol{\Omega}_i(k)$, and $\boldsymbol{T}_i$, the maximum rank $\boldsymbol{B}_i\boldsymbol{\Omega}_i(k)\boldsymbol{T}_i$ is $2N_h$. Therefore, in order to obtain accurate estimations of the unknown flows, in the stochastic approach, stochastic detection and isolation mechanisms must be included.

Stochastic Detection and Isolation Mechanisms

In the stochastic case, by following a similar procedure as employed in the obtaining of the variational estimation model of the deterministic case, from (18), the variational estimation model is given by

$$\begin{aligned} \Delta\hat{x}_i(k+1) = &G_i\Delta\hat{x}_i(k) + H_i\Delta\hat{\psi}_i(k) + \\ &H_{f_i}\Delta\xi_i(k) + \omega_{\Delta i}(k) \\ \Delta\hat{y}_i(k) = &\Delta\hat{x}_i(k) + \nu_{\Delta i}(k), \end{aligned} \tag{28}$$

where $\omega_{\Delta i}(k) = [\omega_{\Delta up_i}(k)\, \omega_{\Delta dn_i}(k)]^\top$ is related to the remaining process noise, $\omega_{\Delta up_i}(k)$ and $\omega_{\Delta dn_i}(k)$ are normally distributed noise with zero mean. Similarly, $\nu_{\Delta i}(k) = [\nu_{\Delta up_i}(k)\, \nu_{\Delta dn_i}(k)]^\top$ is related to the remaining measurement noise, where $\nu_{\Delta up_i}(k)$ and $\nu_{\Delta dn_i}(k)$ are normally distributed noises with zero mean. Similarly to the stochastic estimation mechanism, in order to consider the expected values of the level variations over an estimation window, the variational model (28) is presented under the following assumption.

Assumption 3 (Expected estimated variations)**.** *Over the estimation window, the expected values of $\Delta\boldsymbol{y}_i$ can be estimated from*

$$\begin{aligned} \Delta\hat{\bar{\boldsymbol{y}}}_i = &\boldsymbol{\Phi}_i\Delta\hat{x}_i(N_{hp} \mid N_{hp}) + \boldsymbol{B}_i\boldsymbol{T}_i\Delta\hat{\bar{\psi}}_i(k) \\ &+ \boldsymbol{B}_{f_i}\Delta\boldsymbol{\xi}_i(k) + \boldsymbol{w}_{\Delta_i}(k) + \boldsymbol{n}_{\Delta_i}, \end{aligned}$$

where $\Delta\hat{\bar{\boldsymbol{y}}}_i \in \mathbb{R}^{2N_h}$ is the vector of estimated expected values of the output variations, and

$$\Delta\hat{\bar{\psi}}_i(k) = [\Delta\hat{\bar{q}}_{tr_i}(k)\, \Delta\hat{\bar{s}}_{up_i}(k)\, \Delta\hat{\bar{s}}_{dn_i}(k)]^\top,$$

is the vector of expected values of the unknown flows variations. Finally, $\boldsymbol{w}_{\Delta_i}(k) \in \mathbb{R}^{2N_h}$ and $\boldsymbol{n}_{\Delta_i} \in \mathbb{R}^{2N_h}$ are the corresponding noise vectors.

In the same way as in (22), the process covariance can be modeled as

$$P_{\Delta_i}(k+1) = G_i P_{\Delta_i}(k) G_i^\top + R_\Delta + S_\Delta.$$

Note that the measurement and process noises at different time instants are not correlated (i.e., there is no correlation between $\omega_i(k)$ and $\omega_i(k-1)$, and $\nu_i(k)$ and $\nu_i(k-1)$). Therefore, the noise standard deviations of $\omega_{\Delta up_i}(k)$, $\omega_{\Delta dn_i}(k)$, $\nu_{\Delta up_i}(k)$, and $\nu_{\Delta dn_i}(k)$ are given by $2\sigma_{\omega up_i}$, $2\sigma_{\omega dn_i}$, $2\sigma_{\nu up_i}$, and $2\sigma_{\nu dn_i}$, respectively. Hence,

$$R_\Delta = \begin{bmatrix} 2\sigma^2_{\omega up_i} & 0 \\ 0 & 2\sigma^2_{\omega dn_i} \end{bmatrix}, \; S = \begin{bmatrix} 2\sigma^2_{\nu up_i} & 0 \\ 0 & 2\sigma^2_{\nu dn_i} \end{bmatrix}.$$

As a result, the process covariance ($\boldsymbol{\Sigma}_{\Delta_i}(k) \in \mathbb{R}^{3N_h\times 3N_h}$) can be calculated yielding to a diagonal matrix of the form

$$\begin{aligned} \boldsymbol{\Sigma}_{\Delta_i}(k) = &\text{diag}(P_{\Delta_i}(N_{hp} \mid N_{hp}), \\ &P_{\Delta_i}(N_{hp}+1 \mid N_{hp}), \\ &\cdots \quad P_{\Delta_i}(k \mid N_{hp})). \end{aligned} \tag{29}$$

Consequently, following the same procedure to obtain (26), the estimation of the unknown flow variation, can be reached by minimizing the following objective function

$$\boldsymbol{J}_{\boldsymbol{s_i}} = \|\boldsymbol{\Delta y}_i - \boldsymbol{\Delta}\hat{\bar{\boldsymbol{y}}}_i\|^2_{\boldsymbol{\Sigma}_{\Delta_i}(k)^{-1}} + \|\Delta\hat{\bar{\psi}}_i(k-1) - \Delta\hat{\bar{\psi}}_i(k)\|^2_{\mathcal{D}_{s_i}}, \tag{30}$$

where $\mathcal{D}_{s_i} \in \mathbb{R}^{3\times 3}$ penalize the forgetting factor.

Likewise as in the deterministic case, in the stochastic case, the isolation mechanism uses the estimation of the expected unknown flow variations to establish the origin of the unknown flow and to penalize the corresponding forgetting factor of the estimation mechanism.

IV. CASE STUDY

The proposed deterministic and stochastic strategies are tested using the benchmark based on the Corning canal in California, which has been presented in [19] and the ASCE Task Committee on Canal Automation Algorithms as a standardized testbed on canals with well-studied and realistic properties.

The testbed has been implemented in the storm water management model (SWMM), developed by the United States Environmental Protection Agency (EPA), which numerically solves the SVE of the implemented testbed. The implementation is presented in Fig 7. Even though the testbed is composed by eight channels, since the estimation strategies present the same structure for any channel, the simulation is limited to only one channel (the first channel of the testbed in Figure 7). This is a rectangular channel with the following dimensions: length of 7000m, width of 7m, upstream elevation of 4.4m, and downstream elevation of 3.29m. As it is highlighted in Fig. 7, in the first channel, in order to emulate the unknown flows to be detected and estimated, two orifices with variable areas from 0 to 0.04m^2 have been included. A more detailed description of the design and implementation process follows.

A. SAMPLING TIME

Although most of the OCIS are large-scale systems with very slow dynamics, it has been observed that the time response of the system variation can be almost ten times faster than the system dynamics. Therefore, in order to capture the dynamics of the system variation, the sampling time has been selected by analysis of the time response level variation. In this analysis, the classical control rule of choosing a sampling time ten times smaller than the rise time [23] is used, yielding to a sampling time of $\tau_s = 100\text{s}$.

B. MODEL AREAS

The model areas have been found by using data fitting (7), with the constraint given by $a_{up_1} + a_{dn_1} = 49000$, obtaining upstream and downstream areas given by $a_{up_1} = 21864\text{m}^2$ and $a_{dn_1} = 27136\text{m}^2$.

C. NOISE AND LOW-PASS FILTER

As it is shown in [34], there is a close relationship between the measurement noise standard deviation and the sensor quality. In this case study, it is considered that in OCIS, levels are measured with ultrasound sensors, and according to the quality of the commercial sensors, the measurement noise standard deviation could be between $1 \times 10^{-3}\text{m}$ and $2.5 \times 10^{-3}\text{m}$. Therefore, the deterministic and stochastic algorithms have been tested with measurements obtained from the testbed implemented in the SWMM, and the measurements have been contaminated with noise of these standard deviations.

Moreover, it must be contemplated that in comparison with the system sampling time (τ_s), the sensor's sampling time should be small. This data availability is exploited with the integration of low-pass filters to reduce the measurement standard deviation. For this reason, a third-order low-pass filter is included with a cutoff frequency of 0.02Hz. This frequency is chosen by using the Nyquist-Shannon sampling theorem, and the selected sampling time of 100s. With the inclusion of the low-pass filter, the standard deviation of the remaining measurement noise is almost ten times lower than the original.

D. WEIGHTING MATRICES

Detection Weighting Matrices of the Deterministic Mechanism

In the deterministic mechanism, for the sake of simplicity, the detection weighting matrices of (16) can be described as $\mathcal{D}_{1_i} = d_{1_i}\boldsymbol{I_{2N_h}}$, and $\mathcal{D}_{2_i} = d_{2_i}\boldsymbol{I_{3N_h}}$, where d_{1_i}, and d_{2_i} are positive weighting constants and $\boldsymbol{I_{2N_h}}$, and $\boldsymbol{I_{3N_h}}$ are identity matrices with dimensions $2N_h \times 2N_h$ and $3N_h \times 3N_h$, respectively. In the deterministic case, the relation between the weighting parameters (d_{1_i}, and d_{2_i}) has been used as a tuning parameter. In the tuning procedure: i) the weighting parameter that penalizes the forgetting factor has been chosen as $d_{2_i} = 1$; and ii) Monte Carlo tests have been developed, where a key performance indicator (KPI) has been established in order to find the value of d_{1_i} that minimizes the detection error of the unknown flows. The KPI that has been established in order to mitigate the noise detection and give strong penalization of large detection errors is given by

$$KPI = \sum_{k=1}^{k_f} \frac{(\Delta s_{up_i}(k) - \Delta\hat{s}_{up_i}(k))^4}{k_f - 1} + \frac{(\Delta s_{dn_i}(k) - \Delta\hat{s}_{dn_i}(k))^4}{k_f - 1}, \tag{31}$$

where k_f is the length of data used in the tests. The tests show that small values of d_{1_i} attenuate the estimation noise, but also increase inaccurate detections. On the other hand, large values of d_{1_i} increase the detection accuracy but also increase the noise detection. The results of the Monte Carlo tests are shown in Fig. 8, where it is observed that d_{1_i} values close to 2×10^5 offer the lowest detection errors.

Estimation Weighting Matrices of the Deterministic Mechanism

Note that in the estimation cost function of the deterministic mechanism (12), the weighting matrix that penalizes the forgetting factor $\mathcal{R}_{2_i}$ is modified by the isolation mechanism. In this mechanism, the parameters α_i and β_i have been selected as $\alpha_i = 1$ and $\beta_i = 1 \times 10^6$, where the arbitrary value of β_i is higher enough to avoid the change of the unlikely flow. On the other hand, the weighting matrix $\mathcal{R}_{1_i}$ has been simplified as $\mathcal{R}_{1_i} = r_{1_i}\boldsymbol{I_{2N_h}}$, where r_{1_i} is a tuning constant. In order to find accurate r_{1_i} values, Monte Carlo tests have been performed. In these tests, the r_{1_i} values are evaluated in order to minimize the mean square error (MSE) between the estimated and measured unknown flows by

$$MSE = \sum_{k=1}^{k_f} \frac{(s_{up_i}(k) - \hat{s}_{up_i}(k))^2}{k_f - 1} + \frac{(s_{dn_i}(k) - \hat{s}_{dn_i}(k))^2}{k_f - 1}. \tag{32}$$

As it is shown in Fig. 9, it has been found that small values of r_{1_i} reduce the noise estimation with an inaccurate estimation of the unknown flows, and large values of r_{1_i} increase the estimation accuracy but also the noise estimation, finding that with r_{1_i} values close to 0.5×10^5, accurate and readable estimations of the unknown flows can be reached.

Weighting Matrices of the Stochastic Mechanism

Note that in the stochastic mechanism, the penalization matrices $\boldsymbol{\Sigma}_i(k)^{-1}$ and $\boldsymbol{\Sigma}_{\Delta_i}(k)^{-1}$ (Equations (26) and (30), respectively), are obtained from the process covariance (23) and (29), where the information about the noise standard deviations ($\sigma_{\nu up_i}$, $\sigma_{\nu dn_i}$, $\sigma_{\omega up_i}$ and $\sigma_{\omega dn_i}$) is required. All the standard deviations have been obtained from system measurements at steady state. $\sigma_{\nu up_i}$, and $\sigma_{\nu dn_i}$ have been estimated directly from the standard deviation of the measured noise. The standard deviations associated to the flows measurements ($\sigma_{\omega up_i}$ and $\sigma_{\omega dn_i}$) have been estimated using the respective hydraulic relation presented in Table 2, and discretized multiplying by $\frac{\tau_s}{a_{up_i}}$ or $\frac{\tau_s}{a_{dn_i}}$ as appropriate. On the other hand, the forgetting penalization matrices ($\mathcal{D}_{s_i}$ and $\mathcal{R}_{s_i}(k)$) have been set as $\mathcal{D}_{s_i} = \boldsymbol{I_3}$, and $\mathcal{R}_{s_i}(k)$ is modified by the isolation mechanism with $\alpha_i = 1$ and $\beta_i = 1 \times 10^6$.

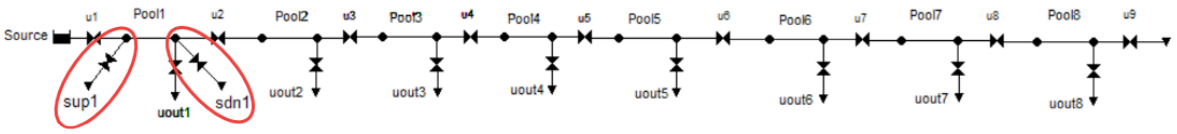

Fig. 7. Case Study simulation in EPA-SWMM.

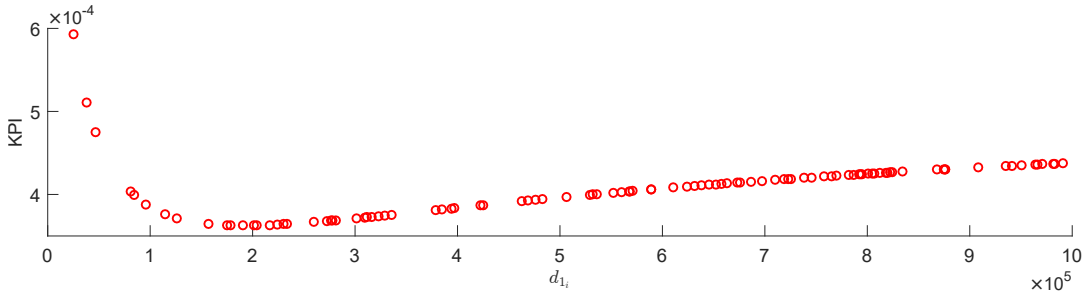

Fig. 8. Monte Carlo tests to establish the d_{1_i} values that offer the lowest detection errors

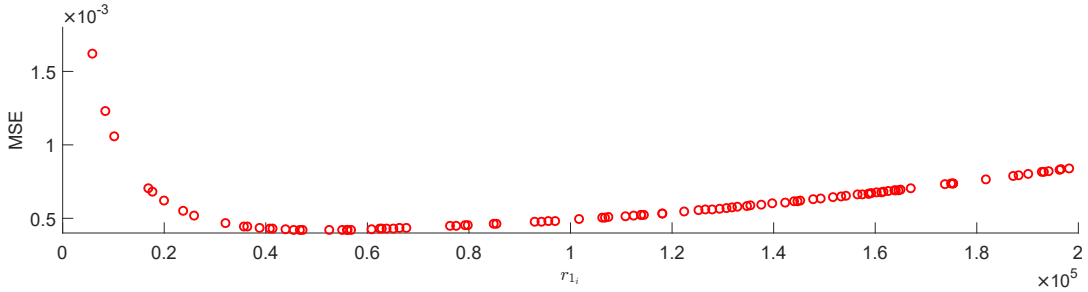

Fig. 9. Monte Carlo tests to establish the r_{1_i} values that offer the lowest estimation errors.

E. ISOLATION MECHANISM THRESHOLD

For the deterministic and stochastic cases, the threshold value has been adjusted from tests of the detection mechanisms at steady state, where the standard deviations of the estimated upstream and downstream unknown flow variations have been used to adjust the threshold value.

As it is shown in Fig. 10, by the development of Monte Carlo tests, it has been found that a threshold value equal to 4.5 times the maximum standard deviation of the estimated upstream and downstream unknown flow variations avoids false detections and allows unknown flows detections.

F. IMPLEMENTATION

Finally, the deterministic and stochastic approaches are implemented by using the algorithms 1, and 2 respectively. In these algorithms, the f_l variable has been included to prevent false triggering of the stochastic and deterministic detection mechanisms.

V. SIMULATION RESULTS AND DISCUSSION

In the simulation results, the deterministic and stochastic approaches are contrasted using filtered measurement noise, where a noise attenuation close to 20dB is obtained. Therefore, in order to test the approaches in the highest and lowest measurement noise scenarios, first, the approaches are contrasted with a filtered measurement noise with a standard deviation of 1×10^{-4}m; and second, the approaches are contrasted with a filtered measurement noise with a standard deviation of 2.7×10^{-4}m.

A. EVALUATION FOR THE SMALLEST NOISE CASE

Figure 11 shows the performance comparison of the deterministic and stochastic detection mechanisms, where it is observed that when an unknown flow variation occurs, both approaches present estimated upstream and downstream unknown flows variations. Also, as expected, the stochastic mechanism presents the lowest noise amplitude. Additionally, in both cases, it is observed small false detections that account for the upstream and downstream levels interactions. Figure 12 shows the operation mode of the deterministic and stochastic isolation mechanisms, where the threshold Λ_{Δ_1} is established at six times the maximum experimental standard deviations between $\Delta\hat{s}_{up_1}$ and $\Delta\hat{s}_{dn_1}$. Therefore, only detections that overcome the threshold value are used to establish the origin of the unknown flow and change the corresponding forgetting factor. In Fig. 12, the deterministic and stochastic strategies present similar behavior. However, the relations between the maximum detected variation and the threshold of the deterministic and stochastic approaches are close to 3.8 and 6.6, respectively. That means that the stochastic detection mechanism offers a better relationship between the estimated signal and the estimated noise. Therefore, with the stochastic mechanism, it is most likely to detect unknown flows from noisy measurements. In Fig. 13, the behaviors of the deterministic and stochastic estimation mechanisms are shown, where the deterministic mechanism presents more accurate estimations than the stochastic mechanism. It occurs since the deterministic estimation mechanism finds the optimal unknown parameters ($\hat{k}_{tr_1}$, $\hat{k}_{up_1}$, and $\hat{k}_{dn_1}$) for each time instant. On the other hand, in the stochastic approach, over the estimation window, it is found the

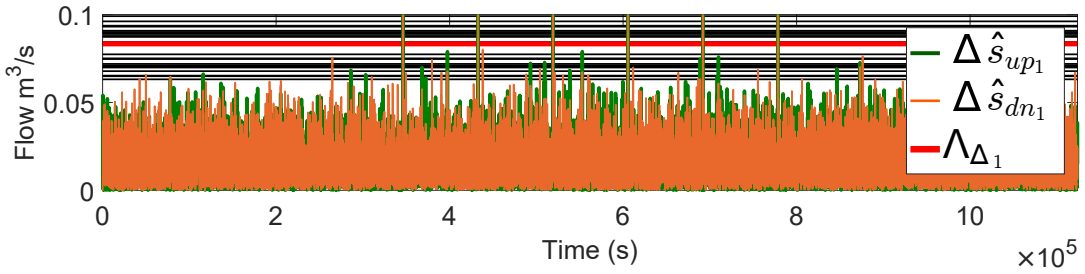

Fig. 10. Monte Carlo tests, where the red line correspond to a threshold value of 4.5 times the maximum standard deviation of the estimated upstream and downstream unknown flow variations.

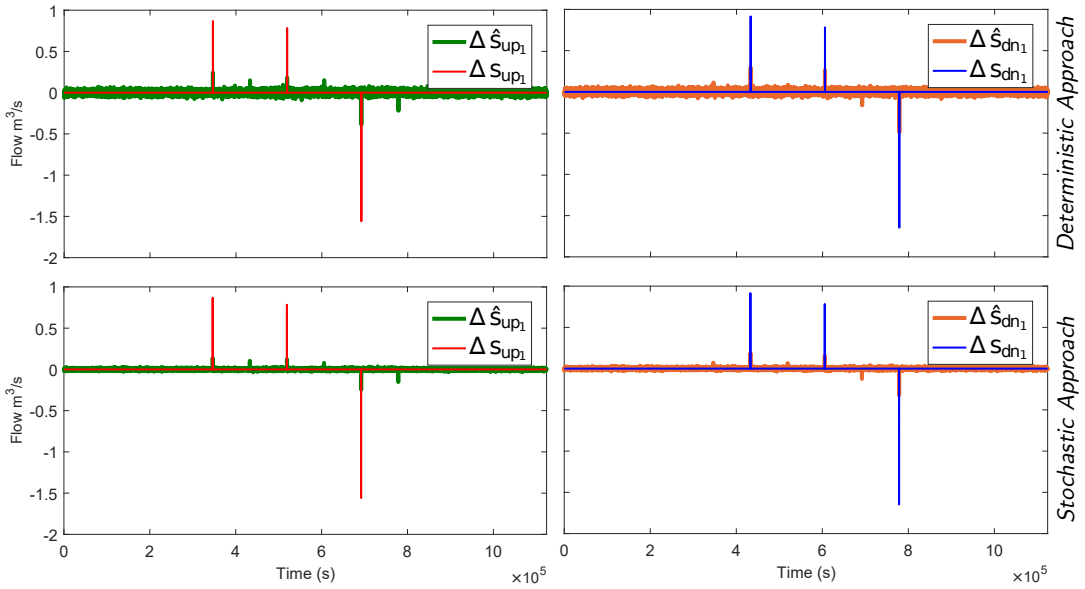

Fig. 11. Performance comparison of the deterministic and stochastic detection mechanisms.

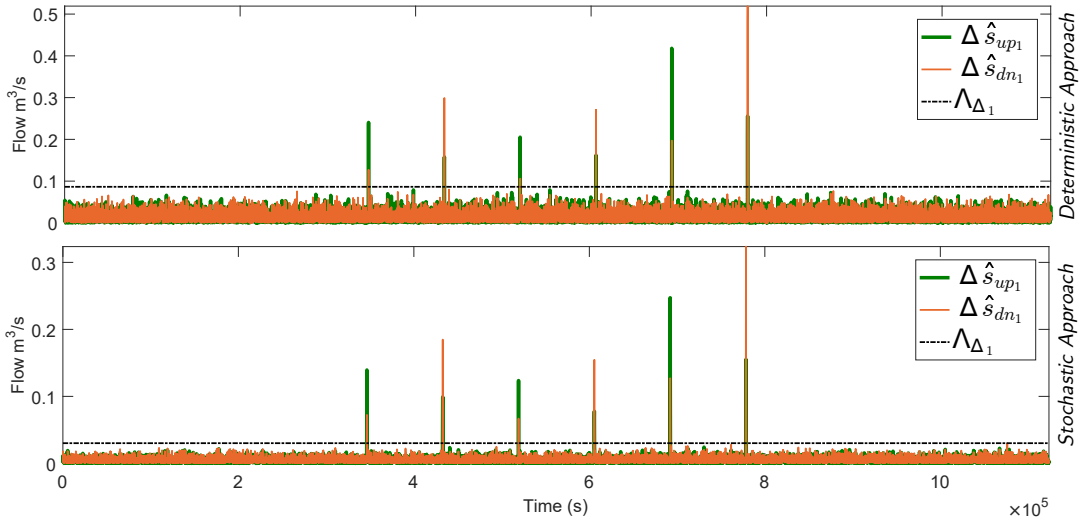

Fig. 12. Comparison of the deterministic and stochastic isolation mechanisms, only detections that overcome Λ_{Δ_1} are compared to establish the origin of the unknown flow.

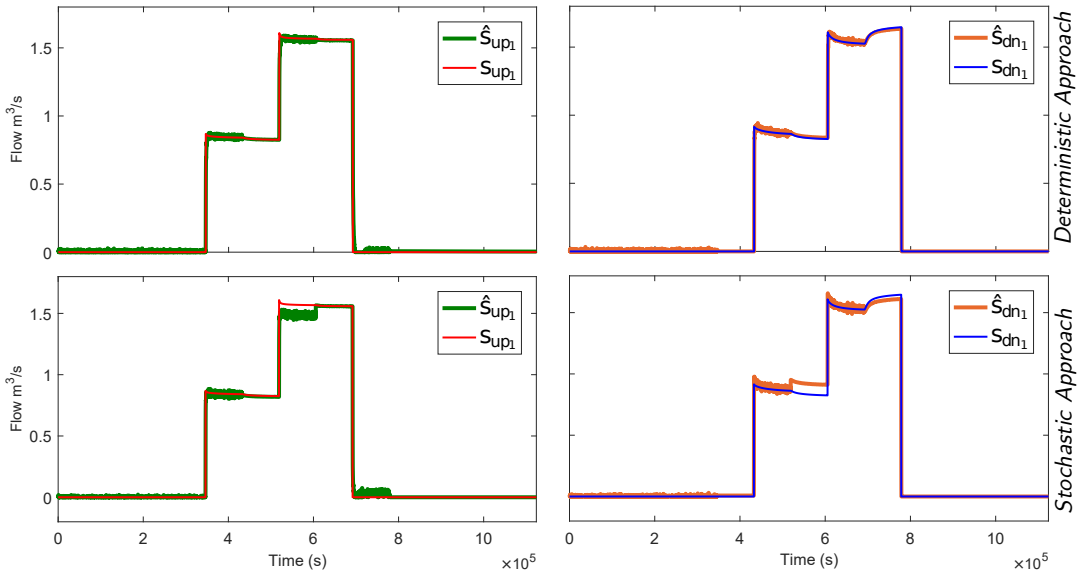

Fig. 13. Performance comparison of the deterministic and stochastic unknown flows estimators.

Algorithm 1 Deterministic estimation algorithm

Define, build, and obtain N_h, $\boldsymbol{\Phi}_i$, $\boldsymbol{B}_i$, $\boldsymbol{B}_{f_i}$, $\mathcal{D}_{1_i}$, $\mathcal{D}_{2_i}$, Λ_{Δ_i}, β_i, α_i, and $\mathcal{R}_{1_i}$.
while estimation is on **do**
  Acquire and evaluate $y_{up_i}(k)$, $y_{dn_i}(k)$, $u_i(k)$, $\xi_i(k)$, $\Delta y_{up_i}(k)$, $\Delta y_{dn_i}(k)$, $\Delta\xi_i(k)$
  if $k > N_h + 1$ **then**
    Obtain $\boldsymbol{y}_i$, $\boldsymbol{\xi}_i(k)$, $\Delta\boldsymbol{y}_i$, $\Delta\boldsymbol{\xi}_i(k)$
    Obtain $\boldsymbol{\Delta\hat{\psi}}$ by minimizing $\boldsymbol{J}_i$
    if $|\Delta\hat{s}_{up_i}(k)| < 0.1\Lambda_{\Delta_i}$ and $|\Delta\hat{s}_{dn_i}(k)| < 0.1\Lambda_{\Delta_i}$ **then**
      $f_l = 0$
    end if
    if $f_l = 0$ and $|\Delta\hat{s}_{up_i}(k)| > \Lambda_{\Delta_i}$ and $|\Delta\hat{s}_{up_i}(k)| > |\Delta\hat{s}_{dn_i}(k)|$ **then**
      $\mathcal{R}_{ktr_i} = \alpha_i, \mathcal{R}_{kup_i} = \alpha_i, \mathcal{R}_{kdn_i} = \beta_i$
    else if $f_l = 0$ and $|\Delta\hat{s}_{dn_i}(k)| > \Lambda_{\Delta_i}$ and $|\Delta\hat{s}_{dn_i}(k)| > |\Delta\hat{s}_{up_i}(k)|$ **then**
      $\mathcal{R}_{ktr_i} = \alpha_i, \mathcal{R}_{kup_i} = \beta_i, \mathcal{R}_{kdn_i} = \alpha_i$
    end if
    Build $\mathcal{R}_{2_i}$
    Obtain $\hat{\boldsymbol{\theta}}_i(k)$ by minimizing $\boldsymbol{V}_i$
    Obtain the unknown flow $\hat{\psi}_i(k) = \Omega_i(k)\hat{\theta}_i(k)$
  end if
end while

Algorithm 2 Stochastic estimation algorithm

Define, build, and obtain N_h, $\boldsymbol{\Phi}_i$, $\boldsymbol{B}_i$, $\boldsymbol{B}_{f_i}$, $\boldsymbol{\Sigma}_{\Delta_i}(k)$, $\mathcal{D}_{s_i}$, Λ_{Δ_i}, β_i, α_i, $\mathcal{R}_{s_i(k)}$, $\omega_i(k)$, $\nu_i(k)$, and $\boldsymbol{T}_i$.
while estimation is on **do**
  Acquire and evaluate $y_{up_i}(k)$, $y_{dn_i}(k)$, $u_i(k)$, $\xi_i(k)$, $\Delta y_{up_i}(k)$, $\Delta y_{dn_i}(k)$, $\Delta\xi_i(k)$
  if $k > N_h + 1$ **then**
    Obtain $\boldsymbol{y}_i$, $\boldsymbol{\xi}_i(k)$, $\Delta\boldsymbol{y}_i$, $\Delta\boldsymbol{\xi}_i(k)$
    Obtain $\Delta\hat{\psi}_i(k)$ by minimizing $\boldsymbol{J}_{\boldsymbol{s_i}}$
    if $|\Delta\hat{\hat{s}}_{up_i}(k)| < 0.1\Lambda_{\Delta_i}$ and $|\Delta\hat{\hat{s}}_{dn_i}(k)| < 0.1\Lambda_{\Delta_i}$ **then**
      $f_l = 0$
    end if
    if $f_l = 0$ and $|\Delta\hat{\hat{s}}_{up_i}(k)| > \Lambda_{\Delta_i}$ and $|\Delta\hat{\hat{s}}_{up_i}(k)| > |\Delta\hat{\hat{s}}_{dn_i}(k)|$ **then**
      $\mathcal{R}_{ktr_i} = \alpha_i, \mathcal{R}_{kup_i} = \alpha_i, \mathcal{R}_{kdn_i} = \beta_i$
    else if $f_l = 0$ and $|\Delta\hat{\hat{s}}_{dn_i}(k)| > \Lambda_{\Delta_i}$ and $|\Delta\hat{\hat{s}}_{dn_i}(k)| > |\Delta\hat{\hat{s}}_{up_i}(k)|$ **then**
      $\mathcal{R}_{ktr_i} = \alpha_i, \mathcal{R}_{kup_i} = \beta_i, \mathcal{R}_{kdn_i} = \alpha_i$
    end if
    Build $\mathcal{R}_{s_i}$
    Obtain $\hat{\hat{\theta}}_i(k)$ by minimizing $\boldsymbol{V}_{s_i}$
    Obtain the unknown flow $\hat{\psi}_i(k) = \Omega_i(k)\hat{\hat{\theta}}_i(k)$
  end if
end while

expected value of the unknown parameters, showing difficulties for rapid changes response. However, it is observed that the estimations of the stochastic approach are suitable enough to be used for DIMEUF.

The total amount of the estimated unknown flows and the estimated flow transition are shown in Fig. 14, where both, the deterministic and stochastic strategies present an ideal estimation of the total unknown flows. That means that despite the discrepancies that the upstream and downstream unknown flows may show, the estimation satisfy the overall channel mass balance, and levels and flows discrepancies are compensated with the flow transition. Note that, in order to compensate rapid changes, the flow transition of the deterministic approach presents rapid variations.

The level's estimation of the deterministic and stochastic approaches are similar and accurate (Fig. 15). This result corroborates the suitability of the selected modeling strategy because, despite the downstream level of the reference model changes almost a meter,

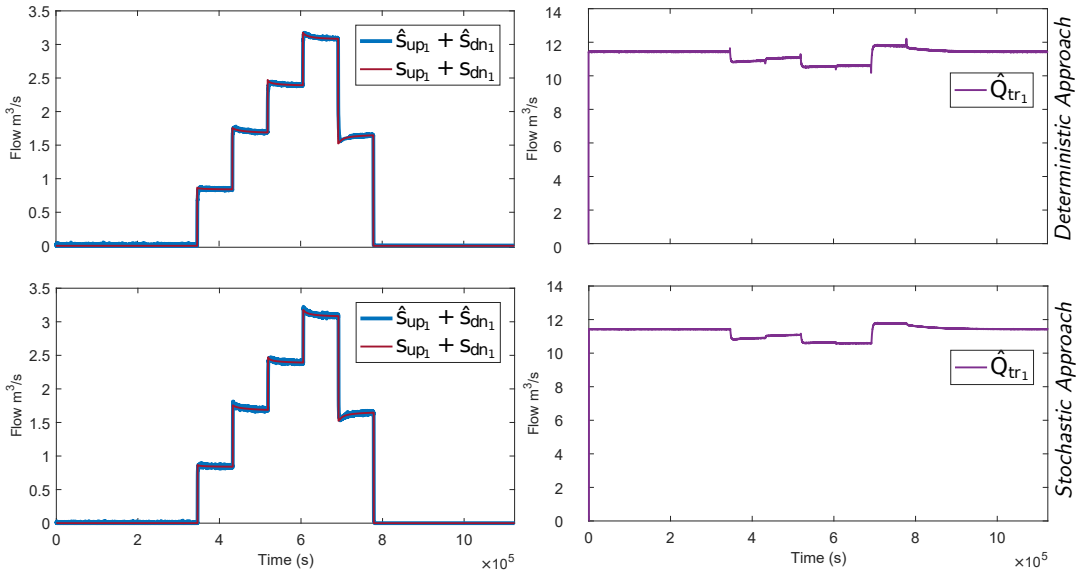

Fig. 14. Total amount of the estimated unknown flows and the estimated flow transition.

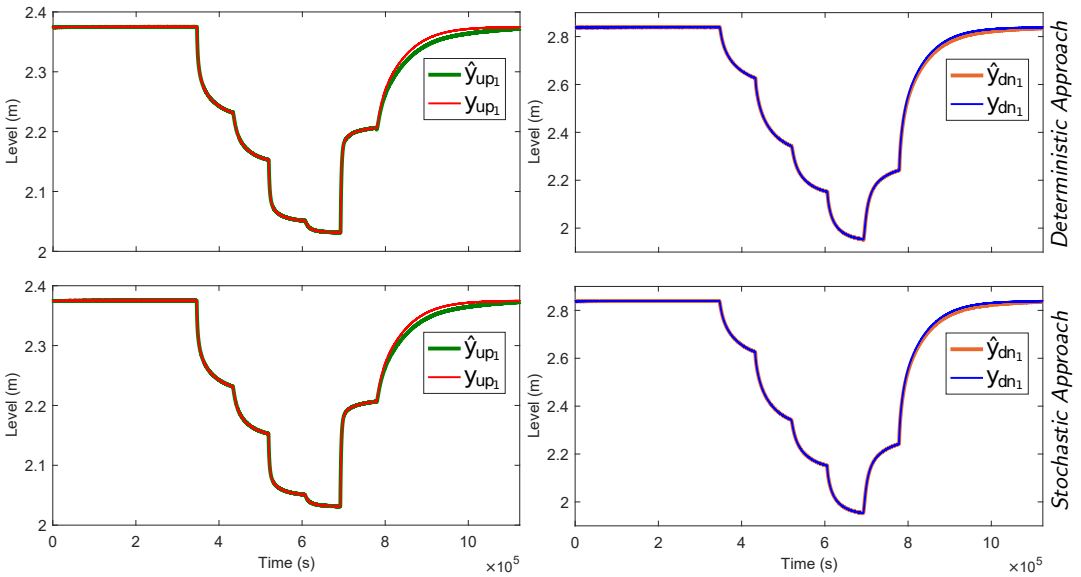

Fig. 15. Levels estimation comparison.

the simplified selected strategy describes accurately the behavior of the system. Moreover, it is highlighted that in the measured and estimated level, the presence of remaining noise is almost imperceptible. This shows one of the hardest problems in the estimation of unknown flows in OCIS, where due to the usual large areas that the OCIS present, even large flow variations can be imperceptible from level measurements, or can be masked between measurement and process noises. For that, next, the behavior of the stochastic and deterministic approaches are tested in presence of highly-noised measurements.

B. EVALUATION FOR THE HIGHEST NOISE CASE

Figure 16 shows the advantage of the stochastic strategy in the detection of unknown flows. In the deterministic strategy, it is observed that there are unreadable unknown flow detections, which are masked for the noise estimation. Similarly, in Fig. 17 it is shown that the deterministic isolation mechanism is not capable of distinguish between the estimated noise and all the estimated unknown flow variations. On the other hand, the stochastic isolation mechanism is capable to accomplish with suitable detections for all variations.

Fig. 18, shows how the isolation problems of the deterministic mechanism induce wrong penalizations and inaccurate estimations of the unknown flows. Conversely, in the stochastic mechanism, the highest noise induce negative effects to the estimation algorithm. However, in the stochastic mechanism, the estimated unknown flows are accurate enough to be used for DIMEUF.

In the deterministic case, the isolation mechanism problems also affect the total estimation flow (Fig. 19), and the estimation of the upstream and downstream levels (Fig. 20). In contrast, the stochastic mechanism only presents small discrepancies in the estimation of the upstream and downstream unknown flows (Fig. 18), highlighting the proper performance of the stochastic strategy in presence of

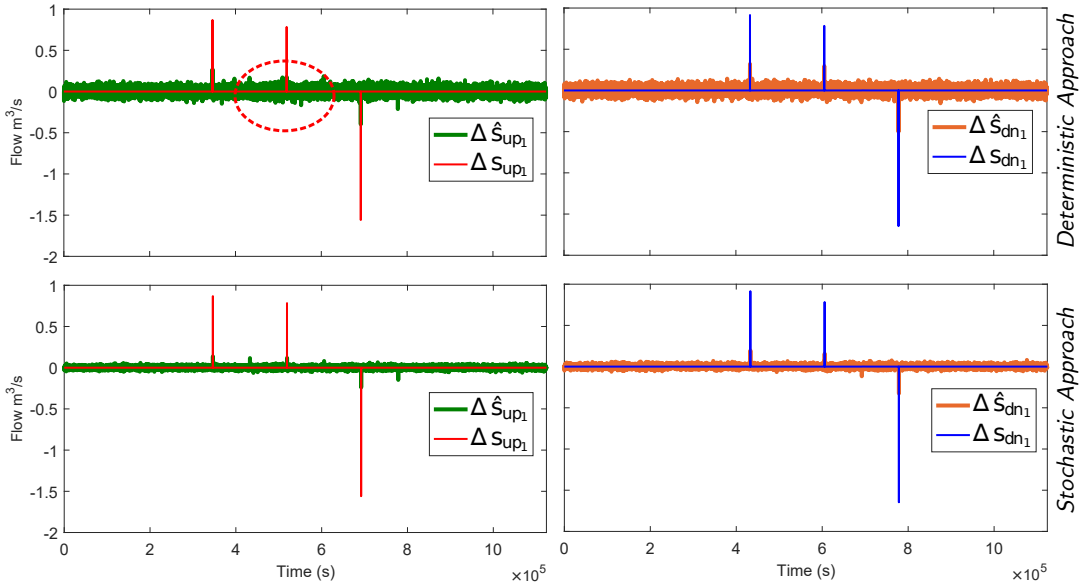

Fig. 16. In presence of highly-noised measurements, it is highlighted that the deterministic detection mechanism presents unreadable unknown flow detections.

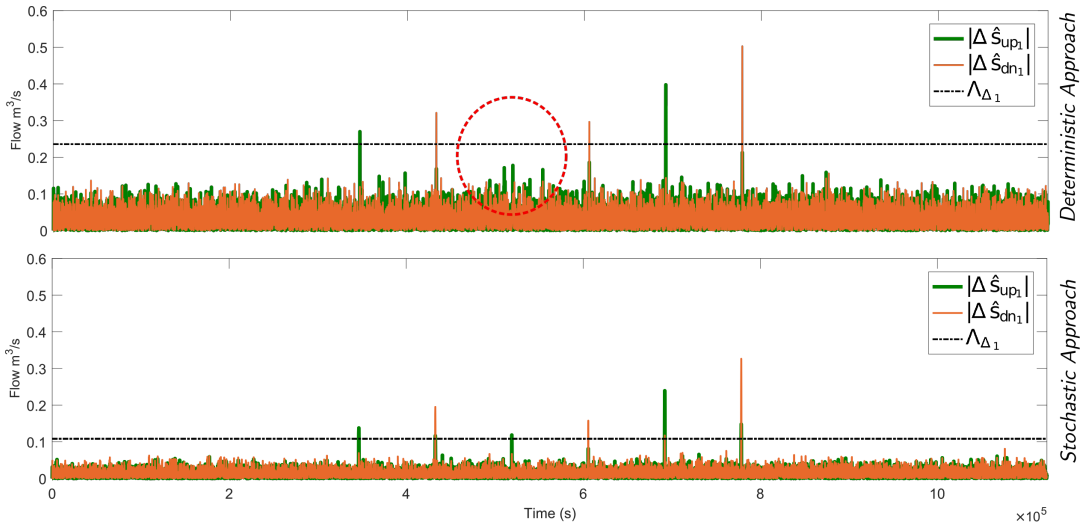

Fig. 17. In presence of highly-noised measurements, it is highlighted that the deterministic isolation mechanism is not capable of distinguish between the estimated noise and all the estimated unknown flow variations.

noisy measurements.

C. UNKNOWN FLOWS ESTIMATION ERRORS COMPARISON

In order to summarize the performance comparison among the deterministic and stochastic approaches under the smallest and highest noise scenarios, Fig. 21 shows the box plots corresponding to distribution data of the upstream plus downstream unknown flows estimation error, where the red lines are the average error value, and the blue lines are first and third quartiles (25^{th} percentile and 75^{th} percentile), showing that even tough the distribution is not normal, in the four cases the error is distributed close to zero. The black lines represent the upstream and downstream limits that contain about 93% of the data, the red marks correspond to the outliers (0.7% of the data). This comparison reveals the advantage of using the stochastic approach (b, d). In the smallest and highest noise scenarios, the data dispersion of the stochastic approach is smaller than the data dispersion presented for the deterministic approach. It must be highlighted that, according to the data distribution, in both scenarios, by using the stochastic approach the estimation precision is increased almost ten times. This finding justifies the use of the stochastic over the deterministic approach.

D. HYDRAULIC CONDITIONS

Despite the developed test has been performed over a realistic system, and the estimation strategies have been contrasted against data obtained from a modeling tool that numerically solves the SVE of the hydraulic systems (obtaining successful results), one question arises over the operative hydraulic conditions of the proposed DIMEUF strategies. Note that the selected simplified modeling

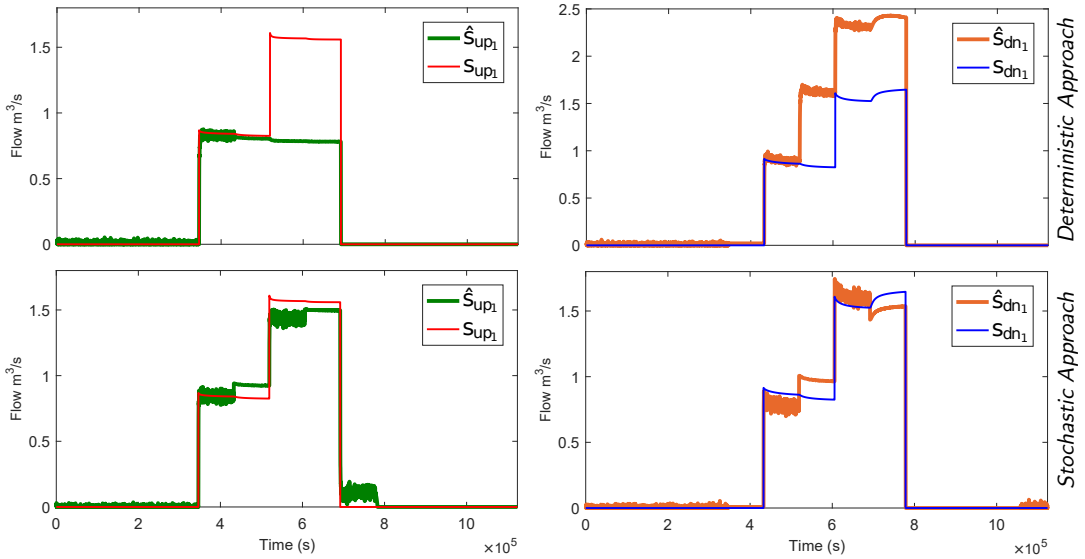

Fig. 18. In presence of highly-noised measurements, the isolation problems of the deterministic mechanism induce wrong penalizations and inaccurate estimations of the unknown flows.

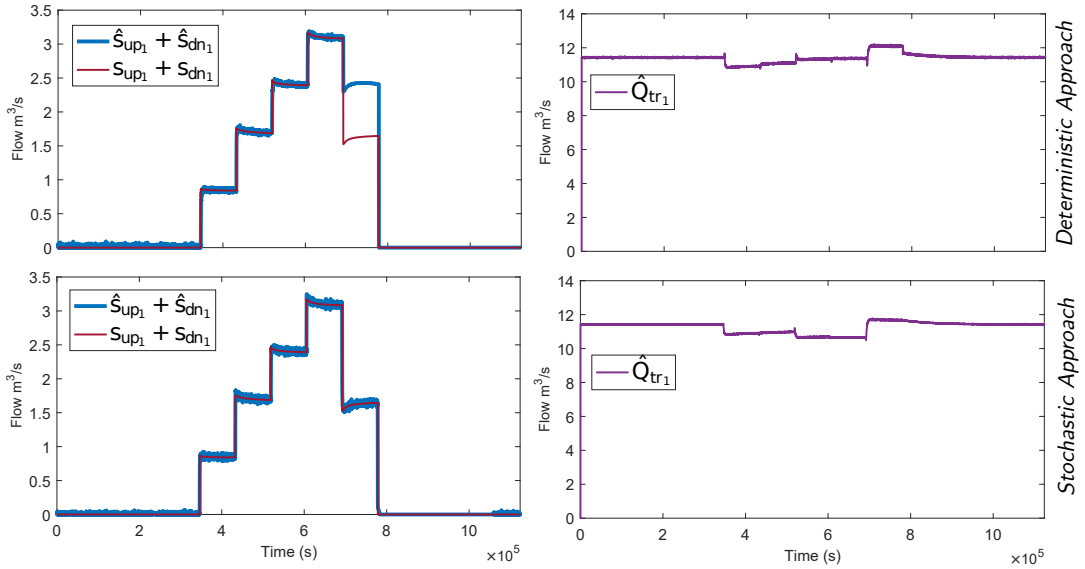

Fig. 19. In presence of highly-noised measurements, the isolation mechanism problems of the deterministic case also affect the total flow estimated.

strategy is the fundamental element of the DIMEUF approaches. Therefore, the operative hydraulic conditions of the estimation strategies can be addressed from hydraulic analyses of the different flows that conform the simplified modeling strategy. With respect to the known channel inflows and outflows, by using the respective flow relations, such as the presented in Table 2, the modeling strategy can be easily adapted to multiple types of hydraulic structures. On the other hand, the flow transition in (2) presents a hydraulic condition that must be analyzed. The flow transition only is real if the head loss due to friction (h_{L_i}) is strictly positive. In that way, the proposed estimation approaches are only useful in OCIS with a considerable potential decay. In order to illustrate this claim, the testings of the estimation strategies using a canal inspired on lateral canal WM of the Maricopa Stanfield Irrigation and Drainage District in central Arizona, reported in [19] is also proposed. This canal is chosen because it presents hydraulic characteristics that are highly different from the characteristics of the Corning canal. The WM canal is a 100m length canal, with upstream elevation of 3.6m, downstream elevation of 3.3m, and width of 1.5m. Moreover, due to the short length of the WM canal, their potential decay can be easily changed by modification of the channel roughness.

In this order of ideas, in Fig. 22, the performance of a stochastic DIMEUF strategy over the WM channel is shown. In this case, the WM channel has been simulated in EPA-SWMM using a Manning roughness coefficient of 0.004 $\mathrm{s/m^{1/3}}$, and the DIMEUF strategy has been designed following the same procedure that had been exposed to the Corning canal. Moreover, in Fig. 22, the behavior of the head loss due to friction is shown. Note that despite the head loss due to friction is small, this is always positive and the DIMEUF strategy reaches an accurate estimation of the unknown

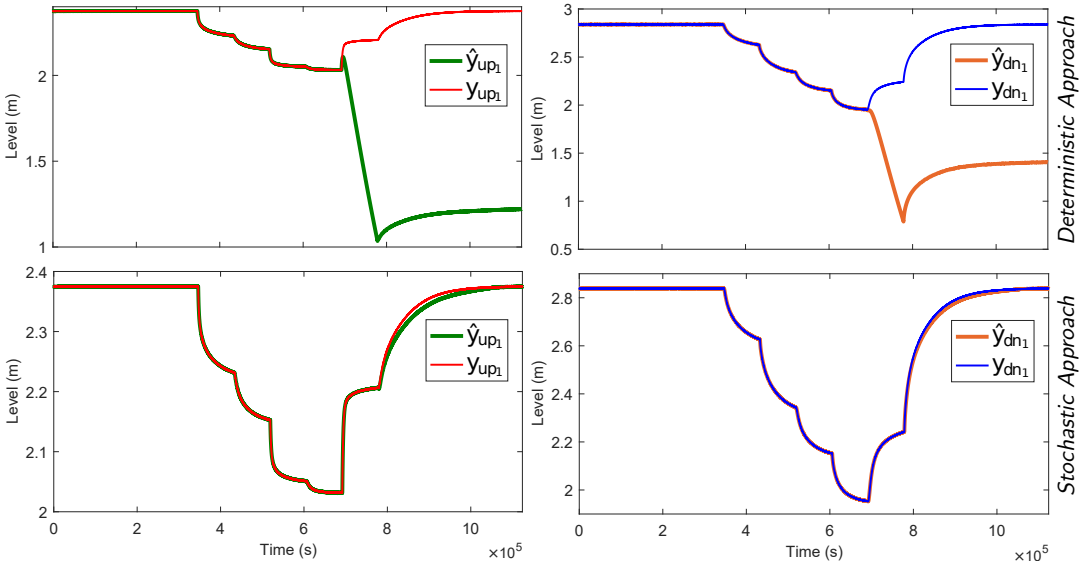

Fig. 20. In presence of highly-noised measurements, the isolation mechanism problems of the deterministic case also affect the estimation of the upstream and downstream levels.

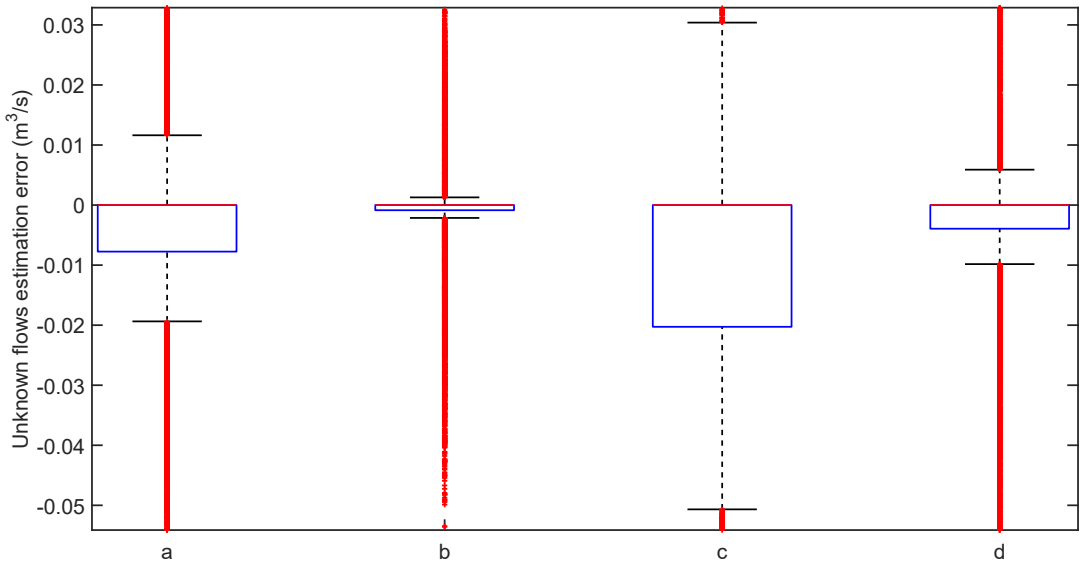

Fig. 21. Comparison of the upstream plus downstream unknown flows estimation error, where: a. corresponds to the evaluation for the smallest noise case of the deterministic approach; b. corresponds to the evaluation for the smallest noise case of the stochastic approach; c. corresponds to the evaluation for the highest noise case of the deterministic approach; and d. corresponds to the evaluation for the highest noise case of the stochastic approach.

flows. On the other hand, in Fig. 22, the head loss due to friction behavior of the WM channel with a Manning roughness coefficient of 0.001 $\mathrm{s/m^{1/3}}$, is shown, where it is observed that the head loss due to friction is close to zero, and there are sections that show negative values of the head loss due to friction. This negative values, which could be attained to the equal mean flow velocity assumption of the approximated model, make impossible the implementation of the developed DIMEUF strategies. This result, which could be interpreted as a limitation of the simplified modeling strategy and therefore of the DIMEUF strategies, can be overcome if, for control and estimation purposes, the channels that have a small head loss due to friction are modeled as a unique storage unit, with area equal to the channel area and known inflows modeled by using the hydraulic relation given in Table 2. In this case, there is a limitation on identifying the either upstream or downstream unknown flow origin, and there is no need to use detection and isolation mechanisms. Another option, which is out of this work scope, could be to eliminate the modeling assumption of an equal mean flow velocity along the channel. This solution implies to use of the SVE in order to establish differential equations that describe the momentum conservation. This information could be used to identify the instant differences between the momentum conservation of the real and modeled systems. Therefore, the development of DIMEUF strategies designed from the SVE have the potential of improving the reached results in this work. However, due to the complexity of the SVE, and the probable model order increases, this development

is not evident.

VI. CONCLUSIONS

In this paper, two strategies for detection isolation and magnitude estimation of unknown flows, which take into account the effects of flow conduction, have been proposed. These strategies have been developed exploiting the advantages that the moving horizon estimation approach has in dealing with constrained non-linear systems. The proposed strategies also take advantage of the forgetting factor, which has been used to incorporate physical information about the most likely unknown flow detected. The strategies have been designed from deterministic and stochastic points of view, showing that including information about noise and expected level values increase the estimation performance. The strategies have been tested using two well-known benchmarks, which have been implemented in an specialized software, showing that although the strategies have been developed using a simplified modeling approach, they are capable of accurately estimate the channel behavior and unknown flows in long operation regions. Into the test, it has been highlighted that due to the nature of the OCIS, in the estimation of unknown flows, the most important challenges to overcome are the measurement and process noise and the uncertainties. For this reason, the real system implementation is an important pending task. Moreover, the integration of the estimation mechanism with control strategies that minimize losses due to unknown flows could be an interesting future direction. Finally, the development of more tests and strategies that mitigate noise detection and estimation impact is an open problem that deserves more attention.

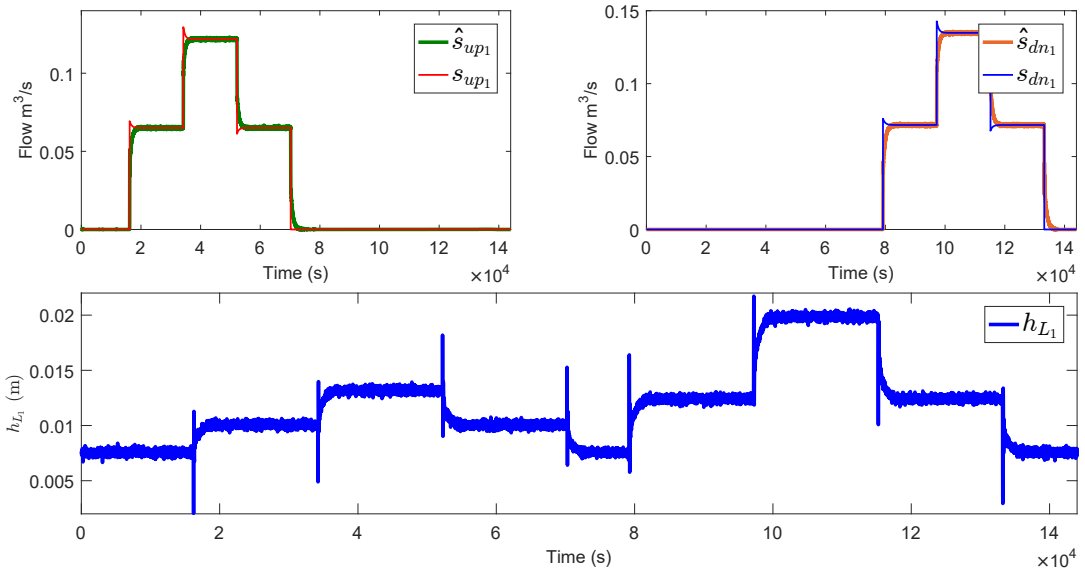

Fig. 22. Head loss due to friction for channel with high roughness coefficient.

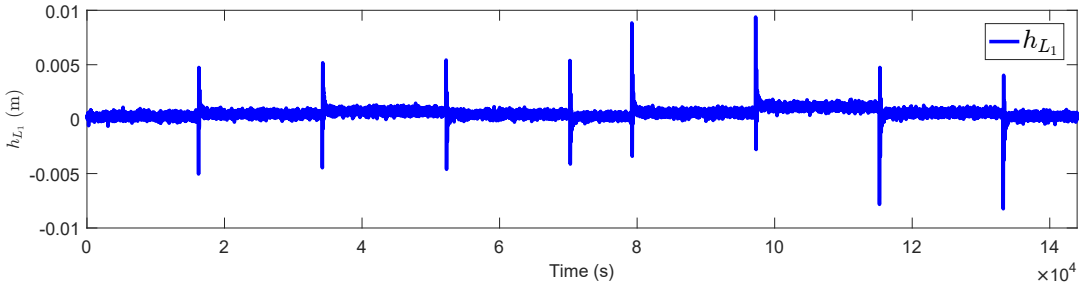

Fig. 23. Head loss due to friction for channel with low roughness coefficient.

TABLE 3. Notation

$i \in \mathbb{Z}$		Stage number (e.g., $i = 1$ denotes the first channel)
p_i		i^{th} channel
$q_i \in \mathbb{R}$	$(\mathrm{m}^3/\mathrm{s})$	p_i inflow
$x_{up_i} \in \mathbb{R}$	(m)	Upstream depth
$x_{dn_i} \in \mathbb{R}$	(m)	Downstream depth
$q_{out_i} \in \mathbb{R}$	$(\mathrm{m}^3/\mathrm{s})$	Outflow to the users
$w_i \in \mathbb{R}$	(m)	Regulation structure width
$g \in \mathbb{R}$	$(\mathrm{m}/\mathrm{s}^2)$	Gravity constant
$c_i \in \mathbb{R}$		Discharge coefficient
$u_i \in \mathbb{R}$	(m)	Regulation structure position
$\kappa_{up_i}(t) \in \mathbb{R}$	$(\mathrm{m}^{2.5}/\mathrm{s})$	Upstream unknown flow parameter
$\kappa_{dn_i}(t) \in \mathbb{R}$	$(\mathrm{m}^{2.5}/\mathrm{s})$	Downstream unknown flow parameter
$a_{up_i} \in \mathbb{R}$	(m^2)	Area of the upstream part of the channel
$a_{dn_i} \in \mathbb{R}$	(m^2)	Area of the downstream part of the channel
$q_{tr_i}(t) \in \mathbb{R}$	$(\mathrm{m}^3/\mathrm{s})$	Flow transition
h_{L_i}	(m)	Head loss due to friction
$z_{up_i} \in \mathbb{R}$	(m)	Upstream elevation
$z_{dn_i} \in \mathbb{R}$	(m)	Downstream elevation
$k_{tr_i}(t) \in \mathbb{R} \in \mathbb{R}$	$(\mathrm{m}^2/\mathrm{s})$	Transition parameter
$\tau_s \in \mathbb{R}$	(s)	Sampling time
$\theta_{a_i} \in \mathbb{R}^2$		Vector of estimated areas
$\phi_{x_i} \in \mathbb{R}^{n-1\times 2}$		Vector of measured variations of levels
$y_{q_i} \in \mathbb{R}^{n-1}$		Vector of measured flows
$\hat{x}_{up_i}(k) \in \mathbb{R}$	(m)	Estimated upstream level
$\hat{x}_{dn_i}(k) \in \mathbb{R}$	(m)	Estimated downstream level
$\hat{q}_{tr_i}(k) \in \mathbb{R}$	$(\mathrm{m}^3/\mathrm{s})$	Estimated flow transition
$\hat{s}_{up_i}(k) \in \mathbb{R}$		Estimated upstream unknown flow parameter
$\hat{s}_{dn_i}(k) \in \mathbb{R}$		Estimated downstream unknown flow parameter
$\hat{x}_i(k) \in \mathbb{R}^2)$		Vector of estimated states
$\hat{\psi}_i(k) \in \mathbb{R}^3$		Vector of estimated unknown flows
$\xi_i(k) \in \mathbb{R}^3)$		Vector of known inputs
$\hat{y}_i(k+1) \in \mathbb{R}^2)$		Vector of estimated outputs
$G_i \in \mathbb{R}^{2\times 2}$		State matrix
$H_i \in \mathbb{R}^{2\times 3}$		Unknown flows matrix
$H_{f_i} \in \mathbb{R}^{2\times 3}$		Known inputs matrix
$\Omega_i(k) \in \mathbb{R}^{3\times 3}$		Matrix of hydraulic relations
$\hat{\theta}_i(k) \in \mathbb{R}^3$		Vector of unknown parameters to be estimated
$\hat{k}_{tr_i}(k) \in \mathbb{R}$		Estimated transition parameter
$\hat{k}_{up_i}(k) \in \mathbb{R}$		Estimated upstream unknown flow parameter
$\hat{k}_{dn_i}(k) \in \mathbb{R}$		Estimated downstream unknown flow parameter
$N_h \in \mathbb{Z}$		Estimation window length
$N_{hp} \in \mathbb{Z}$		Initial position of the estimation window
$\hat{\boldsymbol{y}}_i \in \mathbb{R}^{2N_h}$		Vector of estimated outputs
$\hat{x}_i(N_{hp} \mid N_{hp}) \in \mathbb{R}^2)$		Initial estimated states over the estimation window
$\boldsymbol{\Phi}_i \in \mathbb{R}^{2N_h\times 2}$		State estimation matrix
$\boldsymbol{B}_i \in \mathbb{R}^{2N_h\times 3N_h}$		Unknown flows estimation matrix
$\boldsymbol{\Omega}_i(k) \in \mathbb{R}^{3N_h\times 3N_h}$		Estimation matrix of hydraulic relations
$\hat{\boldsymbol{\theta}}_i(k) \in \mathbb{R}^{3N_h}$		Vector of unknown parameters to be estimated
$\boldsymbol{B}_{f_i} \in \mathbb{R}^{2N_h\times 3N_h}$		Known inputs estimation matrix
$\boldsymbol{\xi}_i(k) \in \mathbb{R}^{3N_h}$		Vector of known inputs
$\boldsymbol{V}_i \in \mathbb{R}$		Estimation cost function
$\boldsymbol{y}_i \in \mathbb{R}$		Vector of measured levels
$\hat{\boldsymbol{\theta}}_i(k-1) \in \mathbb{R}^{3N_h}$		Sequence of unknown parameters estimated in a previous iteration
$\mathcal{R}_{1_i} \in \mathbb{R}^{2N_h\times 2N_h}$		Estimation weighting matrix
$\mathcal{R}_{2_i} \in \mathbb{R}^{3N_h\times 3N_h}$		Estimation weighting matrix
$\nabla^2 \in \mathbb{R}^2$		Hessian operator
$\Delta\hat{x}_i(k) \in \mathbb{R}^2$		Vector of estimated variation of the states
$\Delta\hat{\psi}_i(k) \in \mathbb{R}^3$		Vector of estimated variations of the inputs
$\Delta\xi_i(k) \in \mathbb{R}^3$		Vector of variations of known inputs
$\Delta\hat{y}_i(k+1) \in \mathbb{R}^2$		Vector of estimated variation of the outputs
$\Delta\hat{\boldsymbol{y}}_i \in \mathbb{R}^{2N_h}$		Vector of the estimated variations of the outputs

$\Delta \boldsymbol{y}_{_i} \in \mathbb{R}^{2N_h}$	Vector of the measured variations of the outputs
$\Delta \hat{x}_{_i}(N_{hp} \mid N_{hp}) \in \mathbb{R}^2$	Initial estimated variations of the states
$\Delta \hat{\boldsymbol{\psi}}_i(k) \in \mathbb{R}^{3N_h}$	Vector of the estimated variations of the unknown flows
$\Delta \boldsymbol{\xi}_i(k) \in \mathbb{R}^{3N_h}$	Vector of the known inputs variation
$\boldsymbol{J}_{_i} \in \mathbb{R}$	Detection cost function
$\Delta \hat{\boldsymbol{\psi}}_{_i}(k-1) \in \mathbb{R}^{3N_h}$	Sequence of variations of the unknown flows estimated in a previous iteration
$\mathcal{D}_{1_i} \in \mathbb{R}^{2N_h \times 2N_h}$	Detection weighting matrix
$\mathcal{D}_{2_i} \in \mathbb{R}^{3N_h \times 3N_h}$	Detection weighting matrix
$\Lambda_{\Delta_i} \in \mathbb{R}^2$	Threshold value
$\mathcal{R}_{ktr_i} \in \mathbb{R}$	Estimation weighting parameter related to the flow transition
$\mathcal{R}_{kup_i} \in \mathbb{R}$	Estimation weighting parameter related to upstream unknown flows
$\mathcal{R}_{kdn_i} \in \mathbb{R}$	Estimation weighting parameter related to downstream unknown flows
$\beta_i \in \mathbb{R}$	Parameter used to avoid the change of the unlikely unknown flow
$\alpha_i \in \mathbb{R}$	Parameter used to avoid the change of the unlikely unknown flow
$\omega_{_i}(k) \in \mathbb{R}^2$	Process estimation noise
$\omega_{up_i}(k) \in \mathbb{R}$	Normally distributed upstream process noise
$\omega_{dn_i}(k) \in \mathbb{R}$	Normally distributed downstream process noise
$\sigma_{\omega up_i} \in \mathbb{R}$	Standard deviation of the upstream process noise
$\sigma_{\omega dn_i} \in \mathbb{R}$	Standard deviation of the downstream process noise
$\nu_{_i}(k) \in \mathbb{R}^2$	Remaining measurement noise
$\nu_{up_i}(k) \in \mathbb{R}$	Upstream remaining measurement noise
$\nu_{dn_i}(k) \in \mathbb{R}$	Downstream remaining measurement noise
$\sigma_{\nu up_i} \in \mathbb{R}$	Standard deviation of the upstream measurement noise
$\sigma_{\nu dn_i} \in \mathbb{R}$	Standard deviation of the downstream measurement noise
$\hat{\hat{\boldsymbol{y}}}_{_i} \in \mathbb{R}^{2N_h}$	Vector of estimated expected values of the output
$\hat{\hat{\theta}}_{_i}(k) \in \mathbb{R}^3$	Vector of the unknown parameters expected values
$\hat{\hat{k}}_{tr_i}(k) \in \mathbb{R}$	Expected value of the estimated transition parameter
$\hat{\hat{k}}_{up_i}(k) \in \mathbb{R}$	Expected value of the estimated upstream unknown flow parameter
$\hat{\hat{k}}_{dn_i}(k) \in \mathbb{R}$	Expected value of the estimated downstream unknown flow parameter
$\boldsymbol{T}_{_i} \in \mathbb{R}^{3N_h \times 3}$	Block of identity matrices
$\boldsymbol{w}_{_i}(k) \in \mathbb{R}^{2N_h}$	Process noise vector
$\boldsymbol{n}_{_i}(k+1) \in \mathbb{R}^{2N_h}$	Measurement noise vector
$e_{_i}(k+1) \in \mathbb{R}^{2N_h}$	Estimation error
$P_{_i}(k+1) \in \mathbb{R}^{2\times 2}$	Process covariance
$R \in \mathbb{R}^{2\times 2}$	Process variance
$S \in \mathbb{R}^{2\times 2}$	Measurement variance
$\boldsymbol{\Sigma}_{_i}(k) \in \mathbb{R}^{2N_h \times 2N_h}$	Process covariance
$\boldsymbol{V}_{s_i} \in \mathbb{R}$	Stochastic estimation cost function
$\omega_{\Delta i}(k) \in \mathbb{R}^2$	Process detection noise
$\nu_{\Delta i}(k) \in \mathbb{R}^2$	Measurement detection noise
$\boldsymbol{w}_{\Delta_i}(k) \in \mathbb{R}^{2N_h}$	Process detection noise vector
$\boldsymbol{n}_{\Delta_i}(k+1) \in \mathbb{R}^{2N_h}$	Process measurement noise vector
$P_{\Delta_i}(k+1) \in \mathbb{R}^{2\times 2}$	Process detection covariance
$R_{\Delta} \in \mathbb{R}^{2\times 2}$	Process detection variance
$S_{\Delta} \in \mathbb{R}^{2\times 2}$	Process detection covariance
$\boldsymbol{\Sigma}_{\Delta_i}(k) \in \mathbb{R}^{2N_h \times 2N_h}$	Process detection covariance

REFERENCES

[1] X. Litrico and D. Georges, "Robust continuous time and discrete time flow control of a dam river system. (II) Controller design," Applied Mathematical Modelling, vol. 23, no. 11, pp. 829–846, nov 1999.

[2] P. Swamee, G. Mishra, and B. Chahar, "Design of minimum water-loss canal sections," Journal of Hydraulic Research, vol. 40, no. 2, pp. 215–220, 2002.

[3] D. Koenig, N. Bedjaoui, and X. Litrico, "Unknown input observers design for time-delay systems application to an open-channel," in Proceedings of the 44th IEEE Conference on Decision and Control, 2005, pp. 5794–5799.

[4] N. Bedjaoui, X. Litrico, D. Koenig, and P. O. Malaterre, "H_∞ observer for time-delay systems application to FDI for irrigation canals," in Proceedings of the IEEE Conference on Decision and Control, 2006, pp. 532–537.

[5] E. Weyer and G. Bastin, "Leak detection in open water channels," in Proceedings of the 17th World Congress, vol. 17, no. 1 PART 1. Seoul: IFAC, 2008, pp. 7913–7918.

[6] N. Bedjaoui, X. Litrico, D. Koenig, J. Ribot-Bruno, and P.-O. Malaterre, "Static and dynamic data reconciliation for an irrigation canal," Journal of Irrigation and Drainage Engineering, vol. 134, no. 6, pp. 778–787, 2008.

[7] N. Bedjaoui, E. Weyer, and G. Bastin, "Methods for the localization of a leak in open water channels," Networks and Heterogeneous Media, vol. 4, no. 2, pp. 189–210, 2009.

[8] J. Blesa, V. Puig, and Y. Bolea, "Fault detection using interval LPV models in an open-flow canal," Control Engineering Practice, vol. 18, no. 5, pp. 460–470, 2010.

[9] N. Bedjaoui and E. Weyer, "Algorithms for leak detection, estimation, isolation and localization in open water channels," Control Engineering Practice, vol. 19, no. 6, pp. 564–573, 2011.

[10] O. L. Pocher, E. Duviella, L. Bako, and K. Chuquet, "Sensor fault detection of a real undershot/overshot gate based on physical and nonlinear black-box models," Proceedings of the I8th IFAC Symposium on Fault Detection, Supervision and Safety of Technical Processes, vol. 45, no. 20, pp. 1083–1088, 2012.

[11] S. Amin, X. Litrico, S. Sastry, and A. Bayen, "Cyber security of water SCADA systems-part I: Analysis and experimentation of stealthy deception attacks," IEEE Transactions on Control Systems Technology, vol. 21, no. 5, pp. 1963–1970, 2013.

[12] A. Akhenak, E. Duviella, L. Bako, and S. Lecoeuche, "Online fault diagnosis using recursive subspace identification: Application to a dam-gallery open channel system," Control Engineering Practice, vol. 21, no. 6, pp. 797–806, 2013.

[13] E. Duviella, L. Rajaoarisoa, J. Blesa, and K. Chuquet, "Fault Detection and Isolation of inland navigation channel: Application to the Cuinchy-Fontinettes reach," in Proceedings of the 52nd IEEE Conference on Decision and Control, 2013, pp. 4877–4882.

[14] K. Horváth, J. Blesa, E. Duviella, L. Rajaoarisoa, V. Puig, and K. Chuquet, "Sensor fault diagnosis of inland navigation system using physical model and pattern recognition approach," Proceedings of the 19th IFAC World Congress, vol. 47, no. 3, pp. 5309–5314, 2014.

[15] P. Segovia, J. Blesa, E. Duviella, L. Rajaoarisoa, F. Nejjari, and V. Puig, "Sliding window assessment for sensor fault model-based diagnosis in inland waterways," Proceedings of the 1st IFAC Workshop on Integrated Assessment Modelling for Environmental Systems IAMES 2018, vol. 51, no. 5, pp. 31–36, 2018.

[16] S. Amin, X. Litrico, S. Sastry, and A. Bayen, "Cyber security of water SCADA systems-part II: Attack detection using enhanced hydrodynamic models," IEEE Transactions on Control Systems Technology, vol. 21, no. 5, pp. 1679–1693, 2013.

[17] G. Conde, N. Quijano, and C. Ocampo-Martinez, "Control-oriented modeling approach for open channel irrigation systems," in Proceedings of the IFAC 21s World Congress, Berlin, Germany, 2020, pp. 16 630–16 635.

[18] L. Zou, Z. Wang, J. Hu, and Q.-L. Han, "Moving horizon estimation meets multi-sensor information fusion: Development, opportunities and challenges," Information Fusion, vol. 60, pp. 1–10, 2020.

[19] A. Clemmens, T. Kacerek, B. Grawitz, and W. Schuurmans, "Test cases for canal control algorithms," Journal of Irrigation and Drainage Engineering, vol. 124, pp. 23–30, 1998.

[20] M. Chaudhry, Open-channel flow, 2nd ed. Columbia: Springer Science+Business Media, 2008.

[21] T. Rabbani, F. Di Meglio, X. Litrico, and A. Bayen, "Feed-forward control of open channel flow using differential flatness," IEEE Transactions on Control Systems Technology, vol. 18, no. 1, pp. 213–221, 2010.

[22] G. Conde, N. Quijano, and C. Ocampo-Martinez, "Modeling and control in open-channel irrigation systems: A review," Annual Reviews in Control, vol. 51, pp. 153–171, 2021.

[23] X. Litrico and V. Fromion, Modeling and control of hydrosystems. London: Springer, 2009.

[24] U. S. Department of the Interior, Water measurement manual. Washington, DC: U.S. Government Printing Office, 2001.

[25] M. E. Harr, Groundwater and Seepage, ser. Dover Civil and Mechanical Engineering Series. Dover, 1991.

[26] A. Alessandri, M. Baglietto, and G. Battistelli, "Moving-horizon state estimation for nonlinear discrete-time systems: New stability results and approximation schemes," Automatica, vol. 44, no. 7, pp. 1753–1765, 2008.

[27] J. Baillieul and T. Samad, Encyclopedia of systems and control. London: Springer International Publishing, 2015.

[28] J. B. Rawlings, D. Q. Mayne, and M. Diehl, Model Predictive Control: Theory, Computation, and Design. Nob Hill Publishing, 2017.

[29] R. Bhatia, Positive Definite Matrices. Princeton University Press, 2015.

[30] G. Conde, N. Quijano, and C. Ocampo-Martinez, "An unknown input moving horizon estimator for open channel irrigation systems," in Proceedings of the European Control Conference (To appear), 2021.

[31] M. Darouach and M. Zasadzinski, "Unbiased minimum variance estimation for systems with unknown exogenous inputs," Automatica, vol. 33, no. 4, pp. 717–719, 1997.

[32] A. Alessandri, M. Baglietto, and G. Battistelli, "Design of state estimators for uncertain linear systems using quadratic boundedness," Automatica, vol. 42, no. 3, pp. 497–502, 2006.

[33] M. Verhaegen and V. Verdult, Filtering and System Identification: A Least Squares Approach. Cambridge University Press, 2007.

[34] B. Wahlin and D. Zimbelman, Canal automation for irrigation systems. WEST Consultants, Tempe, AZ, United States: American Society of Civil Engineers (ASCE), 2014, vol. 67, no. 1.